LOS ALAMOS SCIENTIFIC LABORATORY
of the
University of California
LOS ALAMOS • NEW MEXICO

A Risk Analysis of the
Omega West Reactor

by

Harry J. Otway
Morris E. Battat
Ronald K. Lohrding
Robert D. Turner
Richard L. Cubitt

A RISK ANALYSIS OF THE OMEGA WEST REACTOR

by

Harry J. Otway, Morris E. Battat, Ronald K. Lohrding,
Robert D. Turner, and Richard L. Cubitt

ABSTRACT

A method for estimating the risk from reactor installations is presented and applied to the Omega West Reactor, an 8-MWth research reactor at Los Alamos, New Mexico.

The method, which considers both accident probabilities and various wind and weather conditions, estimates individual risk as a function of direction and distance from the reactor and estimates the total detriment to the community as the consequence of reactor accidents.

The somatic risk due to thyroid carcinoma from ^{131}I uptake, the somatic risks of leukemia and other neoplasms from whole-body irradiation, the genetic risk, and nonspecific life-shortening were considered. The individual somatic risk at the nearest habitation was found to be 5×10^{-10}/yr, and the total detriment to the community was 4.5×10^{-4} deaths per year of reactor operation.

Statistical treatment of reactor operating history and test data to obtain reliability estimates is outlined. The results of this study are compared with those from analysis of a 3200-MWth pressurized water reactor.

I. Introduction

This work, an attempt to quantify the risk to the Los Alamos community from operation of the Omega West Reactor (OWR), was prompted by a proposal to increase the reactor operating power from 5 to 8 MWth. The OWR is a tank-type research reactor operated by the Los Alamos Scientific Laboratory (LASL) at Los Alamos, New Mexico. A more detailed description is given in Appendix A.

Risk, as used here, is the probability of an individual's meeting a certain fate from a particular cause. Specifically it could be one's probability of meeting death from a reactor accident and would involve the probability of the accident occurring, the probability of radioactive material being carried to one's location, and his probability of dying after receiving the radiation dose. The specific risks considered here are the somatic risk of death (both early and late) from thyroid carcinoma (from ^{131}I) and leukemia and other carcinomas due to whole-body irradiation, the genetic risk, and the risk of nonspecific life-shortening. The method of assessment is a refinement and extension of that described in Refs. 1 and 2.

II. The Method

A. Discussion. The method determines individual risk as a function of distance and direction from the reactor. The risk is the sum of the biological risks from each possible accident weighted by the respective accident probabilities. Identifying each accident sequence is difficult; some predictable accidents may be overlooked and some interactions of systems are unpredictable. However, one can estimate an upper risk limit by analyzing all recognizable accidents and assuming that accident consequence (fission-product release) is a continuous function of accident probability, i.e., an infinite number of accidents. Thus, discrete sets of identifiable and unidentifiable accidents can be conservatively approximated by an infinite number of accidents forming a continuous spectrum. The curve of fission product release vs accident probability based upon a set of recognizable accidents is not a true random sample, but neither is it biased, so this approximation appears reasonable. This curve (Fig. 1) is related to the probability density function of fission-product release and may be called an "accident chain." The accident chain is actually a line bounding the
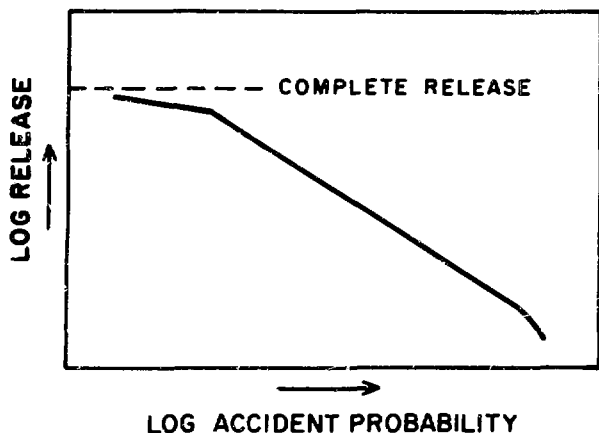
1

Fig. 1.
A typical accident chain.

envelope of accidents; there are also accidents that fall below the line.

As the fission-product release increases, one would expect accident probability to decrease, with the curve asymptotically approaching the limiting value of 100% release at very low probability. Assumption of a continuous accident spectrum is conservative—one or two accidents outside the envelope would not be significant additional risk when added to the integrated area of the envelope. Note that the 90% confidence level shown in Fig. 1 is not a confidence level for all accidents within the envelope, but, rather, only for those accidents that describe the envelope border. For most accidents within the envelope, the 90% confidence limit also falls within the envelope.

B. Determination of Accident Chains. The accident chain may be generated by assessing the probability of a primary system failing in conjunction with the failure of any combination of other systems during the time interval (before or after the primary system failure) in which they would be needed. The fission-product release value for the accident situation assumed constitutes one point on the accident chain. This procedure may be repeated for different combinations of system failures to produce additional points and does not restrict one to consideration of spontaneous failure of a primary system as the initiating event. For example, loss of electrical power or an operator error might initiate failure of the reactor cooling system. One need only assess the probability that power failure or operator error will cause failure of the cooling system in the manner postulated, then use this probability to generate a point on the loss-of-coolant accident chain.

This point-generation procedure may be written as

$$P_a = P_p \prod_{i \in I_1} P_i(\tau) \prod_{j \in I_2} [1 - P_j(\tau)] \quad , \qquad (1)$$

where

P_a = yearly probability of postulated accident,
P_p = yearly probability of primary system failure,
$P_n(\tau)$ = probability of the nth safeguard system's failing to start or spontaneously failing during the time (τ) when its failure would affect the accident outcome,

$$I_1 \cup I_2 = \left\{ 1, 2, \ldots, N \right\} , I_1 \cap I_2 = \emptyset \quad ,$$

I_1 = index set of safeguard systems that fail, and

I_2 = index set of safeguard systems that do not fail.

Because system reliabilities for a specified interval are high (at least 0.99), Eq. (1) may be approximated by

$$P_a \cong P_p \prod_{I_1} P_i(\tau) \quad . \qquad (2)$$

By finding the 90% upper limits for P_p and the $P_i(\tau)$'s in the accident chain and substituting these values into Eq. (2), one can plot an approximate 90% confidence curve. The procedure used to find the 90% upper limits is explained in Appendix B.

C. Radiation Dose vs Accident Probability. Radiation doses received as a function of distance from a postulated fission-product release for various weather conditions can be calculated by established methods. Details of weather conditions and fission-product dispersion calculations are summarized in Appendix C. Given the release-probability relationship determined by the method of Sec. B above, one can form a series of dose vs probability curves for various Pasquill weather conditions and distances from the reactor through knowledge of the dose-distance-weather relationship for each fission-product release value. This calculation will be made for both the whole-body dose, which is mostly due to irradiation from ground-deposited iodine isotopes, and for the thyroid dose due to internal irradiation from iodines deposited in the gland; evacuation of personnel was not considered. This calculation is

$$D_i(p,s) = C(p) d_i(s) \quad , \qquad (3)$$

where

$D_i(p,s)$ = dose (thyroid or whole-body) in rads, a function of probability (p), distance from the reactor (s), and the ith Pasquill weather condition,

$C(p)$ = release in curies, ^{131}I biological equivalent plus associated fission products as a function of probability (p), and

$d_i(s)$ = dose in rads per curie of ^{131}I equivalent plus associated products released at distance s under the ith Pasquill weather condition.

2

D. Individual Mortality Risk vs Accident Probability. Once the relationships of radiation dose vs probability for various Pasquill conditions have been determined for the distances of interest, the relationships correlating mortality risk and dose (see Sec. IV-B) may be used to obtain mortality risk as a function of accident probability for several distances. The method is not restricted to use of the linear risk-dose assumption employed here:

$$M_i(p,s) = D_i(p,s)\, m(p) \quad , \tag{4}$$

where

$M_i(p,s)$ = mortality risk (thyroid or whole-body) for the ith Pasquill condition,

$D_i(p,s)$ = defined by Eq. (3), and

$m(p)$ = mortality risk per rad of radiation (thyroid or whole-body).

E. Individual Risk. The total risk to a person at a specific distance and angle from the reactor may be found by integrating the mortality risk of Eq. (4) over all accident probabilities, then multiplying by the probability density function of the wind direction and Pasquill weather conditions, and summing over all Pasquill conditions. The value thus derived permits one to determine the risk on the basis of local weather conditions or to determine a necessary exclusion area.

$$R(\theta,s) = \sum_{i=1}^{N} \left[\int_0^1 M_i(p,s)\, dp \right] f_i(\theta)\, G_i \quad , \tag{5}$$

where

$R(\theta,s)$ = individual mortality risk per year at distance s and angle θ (thyroid or whole-body),

$M_i(p,s)$ = defined by Eq. (4),

$f_i(\theta)$ = probability density function for wind direction θ under the ith Pasquill condition, and

G_i = probability of the ith Pasquill condition's occurring.

These equations effectively determine the risk as a function of distance, for each Pasquill condition, with the wind assumed to be blowing always in the same direction at the most pessimistic speed. The angular distribution of wind direction for each Pasquill condition is then considered to determine the angular distribution of risk. The risk at every location (θ,s), for each Pasquill condition is then added, each risk being weighted by its percentage of occurrence.

One could also consider the distributions of wind speed, humidity, and temperature, but they probably would not appreciably affect the risk estimate.

F. Total Population Risk. The total risk of deaths per year to the population around the reactor site may be found by integrating the individual risk times the population density over distance and angle from the reactor. This is a discrete function because the population does not occur as a continuum, rather each person is a discrete point. The distance summation limits are from the exclusion boundary out to the point where the population stops; the angle summation limits are clearly from 0 to $360°$.

$$T = \sum_{\theta=0}^{360} \sum_{s=0}^{\infty} R(\theta,s)\, H(\theta,s) \quad , \tag{6}$$

where

T = total risk to the population in deaths per year,

$R(\theta,s)$ = defined in Eq. (5), and

$H(\theta,s)$ = number of people at angle θ and distance s from the reactor.

III. Estimation of Failure Rates

A. Discussion. After one has defined a representative subset of accidents from an assumed accident continuum, the main difficulty is in finding the failure probability of each link of the accident chain. The failure rate for each link must be estimated and transformed to probability using Eq. (B-5) of Appendix B.

Of several ways to estimate failures, the least rigorous is to have someone familiar with the system estimate its failure rate. At best this is a poor method, so when using it we always recorded an extremely pessimistic estimate. Thus, if the study were to be biased, it would be toward higher risk.

Another method is to search the literature to find experimentally determined failure rates. Two obvious problems in this type of estimate are that the component may be similar but not identical to the component of interest, and that the failure rate may have been determined in an environment different from that in which the component of interest operates.

B. Estimation from Reactor Data. A third, mathematically pleasing, method of estimating failure rates is to use data from the operating history of the reactor of interest or similar reactors. This is easy if we assume that the failures are distributed as a Poisson process with gamma-distributed waiting time to failure and independent exponentially distributed inter-arrival times. These

3

assumptions are valid if it can be assumed that maintenance and repair result in no wear-out effect.

The problem of accurately estimating failure rates hinges on obtaining enough operating history of a system and its components. If a component does not fail in 15 yr of operation, can we accurately estimate its failure rate? Probably not, but we can certainly put an upper bound on the failure rate and state what confidence we place on that bound. Take, for example, the electric motor that operates the primary spray system of the OWR. This spray system has been tested 130 times without failure. We can compute the upper confidence limit for its failure rate using Eq. (B-4) of Appendix B. Using the equation to compute a 90% confidence interval, we have

$$P\left[0 \leqslant \nu \leqslant \frac{4.61}{(2)(130)}\right] = 0.90 \quad,$$

$$P\left[0 \leqslant \nu \leqslant 1.75 \times 10^{-2}\right] = 0.90 \quad,$$

where ν is the failure rate for the electric motor. This equation implies that, taking one chance in 10 of being wrong, the failure rate of the electric motor is not greater than 1.75×10^{-2}/demand. Similarly, for a 99.9% confidence interval, we have

$$P\left[0 \leqslant \nu \leqslant 5.2 \times 10^{-2}\right] = 0.999 \quad.$$

Discussed in Appendix D, Sec. 3, is an OWR flapper valve that has been tested 500 times without a failure. Using this information, we can compute a 90% confidence interval of

$$P\left[0 \leqslant \nu \leqslant 4.61 \times 10^{-3}\right] = 0.90$$

and a 99.9% confidence interval of

$$P\left[0 \leqslant \nu \leqslant 1.36 \times 10^{-2}\right] = 0.999 \quad.$$

If we could not find an acceptable failure-rate estimate for a component with no observed failures, we conservatively used the 99.9% upper confidence limit. This estimate has some nice properties. It estimates the failure rate of the component in its working environment (although admittedly not in an accident environment) and is forced to be conservative by use of a 99.9% confidence level as the estimated average failure rate.

The method for estimating failure rates when at least one failure occurs is explained in Eq. (B-5) of Appendix B. Take, for example, the three flow blockage accidents that have occurred in 500 reactor-years (see Appendix E, Sec. 4(b)). The exact estimate of the failure rate is $1 - e^{-\hat{\nu}}$, where $\hat{\nu}$ = failures/years observed = 6.0×10^{-3}/yr. Therefore, the failure rate is $1 - e^{-\hat{\nu}} = 5.98 \times 10^{-3}$. This shows that using $\hat{\nu}$ (Eq. (B-5) of Appendix B) to estimate the failure rate is a good approximation for a process observed for 500 yr. Using the above information, we can now compute an upper confidence limit on the failure rate, using Eq. (B-4) of Appendix B.

IV. Risk

A. The Concept of Risk.* We now attempt to give an appreciation for numerical values of risk by considering the values of some that are commonly accepted. Because the reactor risk discussed here is due to reactor accidents, comparison with other accident risks is helpful. Table 1 shows selected U.S. accident figures from 1966. People are not equally exposed to all these hazards and, indeed, some are not exposed to some hazards at all, but many of these accidents are common in our society, so the risks they provide are representative of the "average" risk to the "average" person.

Accidents providing hazards on the order of 10^{-3} per person per year are uncommon. When a risk approaches this level, immediate action is taken to reduce the hazard. This level of risk is unacceptable to everyone.

At an accident level of 10^{-4} per person per year, people spend money, especially public money, to control the cause. Money is spent for traffic signs and control, and police and fire departments are maintained with public funds. Safety slogans popularized for accidents in this category show an element of fear; e.g., "The life you save may be your own."

Risks at the level of 10^{-5} per person per year are still considered by society. Mothers warn their children about most of these hazards (playing with fire, drowning, firearms, poisons), and some people accept a degree of inconvenience, such as not traveling by air, to avoid them.

TABLE 1

SOME U.S. ACCIDENTAL DEATH STATISTICS FOR 1966 (Ref. 3)

Accident	Total Deaths	Probability of Death/Person/Yr
Motor vehicle	53,041	2.7×10^{-4}
Falls	20,066	1.0×10^{-4}
Fire and explosion	8,084	4.0×10^{-5}
Drowning	5,687	2.8×10^{-5}
Firearms	2,558	1.3×10^{-5}
Poisoning (solids and liquids)	2,283	1.1×10^{-5}
Cataclysm	155	8.0×10^{-7}
Lightning	110	5.5×10^{-7}

---

*This section is based in part upon private communication from R. R. Brownlee of LASL.

Safety slogans for these risks have a precautionary ring: "Never swim alone," "Never point a gun at another person," "Keep medicines out of children's reach."

Accidents with a probability of about 10^{-6} per person per year are not of great concern to the average person. He may be aware of them, but he feels they will never happen to him. Phrases associated with these occurrences have an element of resignation: "Lightning never strikes twice," "An act of God."

Another factor affecting this analysis is that risk assessment seems to be influenced by the number of people dying in an accident and by the amount of accompanying property damage. An automobile accident that kills 10 people on the east coast is considered newsworthy in California–10 people killed in 10 separate accidents are not. The Alaska earthquake of 1964 killed 117 people and caused property damage of about $311 million. The largest commercial airplane crashes (one airplane) kill about 100 people and cause property damage of $5 to 100 million. Reaction to these figures may be compared with that to accidents in which people almost always die singly, such as suffocation, which causes about 1300 deaths each year in the USA.

The intent of this discussion was to point out that there is a general lack of concern about accidents having mortality risks of less than 10^{-6}/yr. This will provide a comparison for evaluation of the results of the OWR risk analysis. A more detailed discussion of accident risks is presented in Refs. 1 and 2.

B. The Risks Considered. To avoid underestimating risks, we assumed that the consequences of irradiation are linear with dose, that there are no threshold or rate effects, and that there is no repair of radiation damage. We do not suggest that these conditions represent reality—only that they provide an upper limit of risk. It is quite clear that threshold, rate, and repair effects do exist and make the actual risks lower than those suggested here. Numerical values of the probability of death per unit dose and the sources of these estimates follow.

1. Whole-Body Somatic Risk. The risks included in whole-body somatic risk are death from leukemia and from carcinomas other than of the thyroid. For doses up to 150 rad, a linear relationship of 30×10^{-6} per person per rad has been used as the probability of death from each of these.[1,4] For higher doses, the response is based upon the acute effects of radiation.[5]

2. Thyroid Carcinoma. Assuming that the product of morbidity and mortality is roughly constant for all ages,[1,4] the chance of death from internal ^{131}I irradiation of the thyroid has been taken as 1×10^{-6} per person per rad.

3. Nonspecific Life-Shortening. After radiation exposure of animal populations, increased mortality is noted which is not associated with any single disease but seems

as though the animals had undergone accelerated physiological aging. Studies on animal groups (mostly mice and rats)[6-12] show varied results. Some have not shown this effect at all, while others[6,7] show life-span reductions ranging from 0.5 to 7.8% per 100 rad. The average result seems to be about 2 to 3% life-span reduction per 100-rad dose. A study of American radiologists[13] indicated a value of 4 to 5% per 100 rad, but the dosimetry was uncertain. Studies of British radiologists and the Japanese bomb survivors[14,15] have been inconclusive. An estimated 7% life-span reduction per 100 rad is used here as an approximate upper limit of risk. This may also be expressed as a mortality probability of 700×10^{-6} per person per rad.

4. Genetic Risk. In predicting genetic risk, the term "genetic death " is used. A genetic death may be defined as the eventual extinction of a gene lineage. This might occur through the reduced fertility or sterility of someone carrying the gene or through stillbirth, abortion, or early embryonic or pre-reproductive death. The term is somewhat misleading in that a genetic death may not represent a somatic death; a genetic death (sterility, for example) may not have an associated corpse. Therefore, calculation of radiation-induced mutation frequency is meaningful only in comparison with natural mutation frequency, discussed below.

(a) Radiation-Induced Mutations. Most radiation mutation data come from studies with mice[16-21] that provide a value of 10^{-7} mutations per gene per rad per germ cell. Japanese human data[22] support this figure, which may also be expressed as 4000×10^{-6} mutations per rad per person. The International Commission on Radiological Protection (ICRP)[23] suggests a higher value of 7200×10^{-6} genetic deaths per rad which is used here as an upper limit. About 2.5% of these mutations would be expected in the first generation.[23]

(b) Natural Mutations. A reasonable estimate of natural mutation frequency of the causal genes is about five mutations per million genes per generation.[23-25]

With 20,000 genes per man, this yields 0.1 mutation per germ cell in each generation, or $200,000 \times 10^{-6}$ natural mutations per person per generation. To preserve genetic equilibrium, the number of genetic deaths must equal the number of mutations; therefore, this figure also represents the natural rate of genetic death per person per generation.

V. Results

The results of applying the method to the OWR are outlined. Details of the calculations are given in the appendixes.

A. Fission-Product Release vs Probability. The source term for this risk assessment is the release-probability envelope shown in Fig. 2. The accidents considered

5

are itemized in detail in Appendix E, and details of the reliability data appear in Appendix D. There are five general sources of system and component reliability data:

1. Component reliability measurements.
2. Reactor operating history.
3. Specific system test data.
4. Largely intuitive assessment of reliability.
5. Calculated reliabilities (e.g., fault tree).

We have used all these although 4 and 5 overlap somewhat. The statistical treatment used to obtain confidence levels and failure probabilities from OWR operating history and test data is detailed in Appendix B.

Note that our source term (Fig. 2) is almost identical to that for a 1000-MWe pressurized water reactor with containment and atmospheric spray and cooling systems.[1,2]

B. Risk vs Distance. Risk vs distance results for different Pasquill weather conditions are shown in Figs. 3 through 5. These curves are the results of the calculations described by the integral portion of Eq. (5)—that is, before the probability of occurrence of the various Pasquill conditions has been included. Dose calculations are explained in Appendix C.

Local meteorology is important in considering the OWR which is located in the bottom of a long, narrow canyon. The local meteorology (see Appendix F) as given by Eq. (5) is applied to Figs. 3 through 5 to produce Fig. 6. This figure shows lines of constant somatic mortality risk (thyroid carcinoma, leukemia, and other carcinomas) superimposed upon a schematic plan of Los Alamos. The warehouse immediately northwest of OWR is the nearest
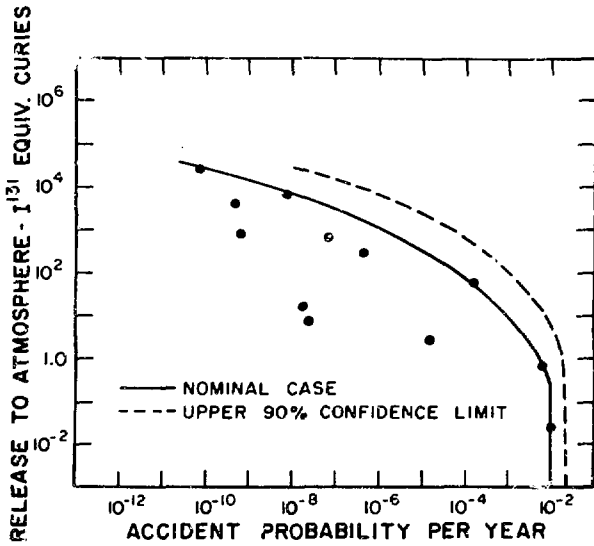

Fig. 3.
Yearly mortality risk vs distance (Pasquill condition Type C, 5m/sec cross-canyon wind).

Fig. 2.
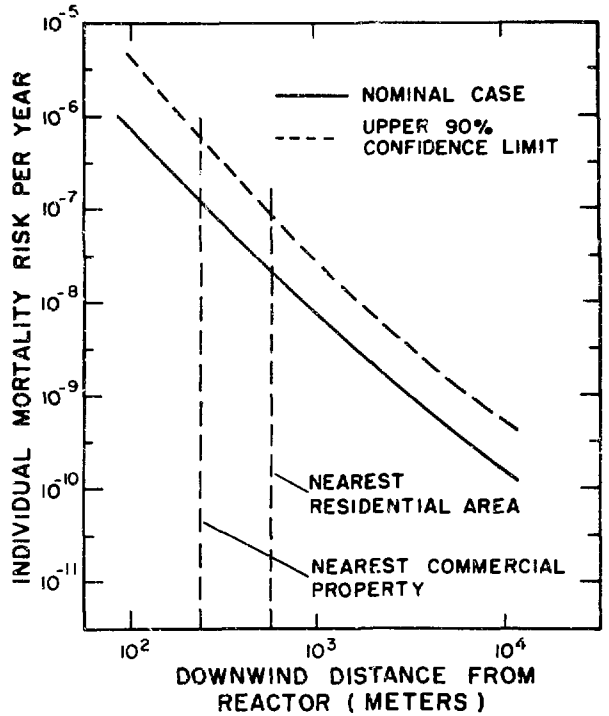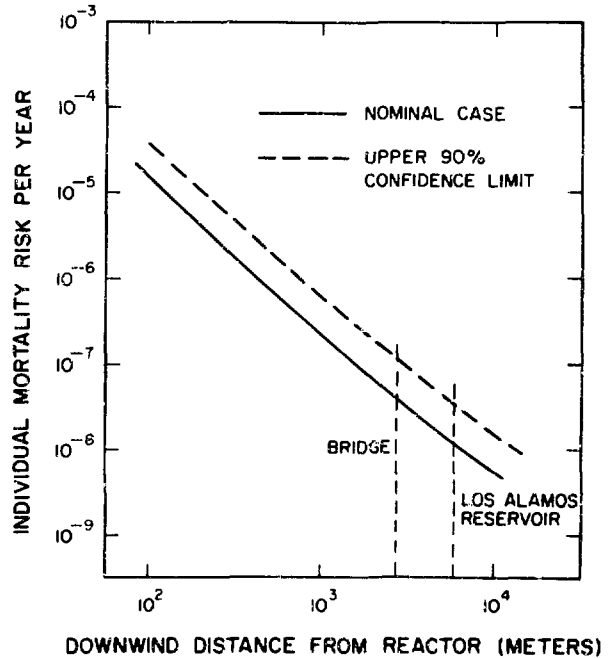*Fission-product release vs probability.*

Fig. 4.
Yearly mortality risk vs distance (Pasquill condition Type E, 1m/sec up-canyon wind).
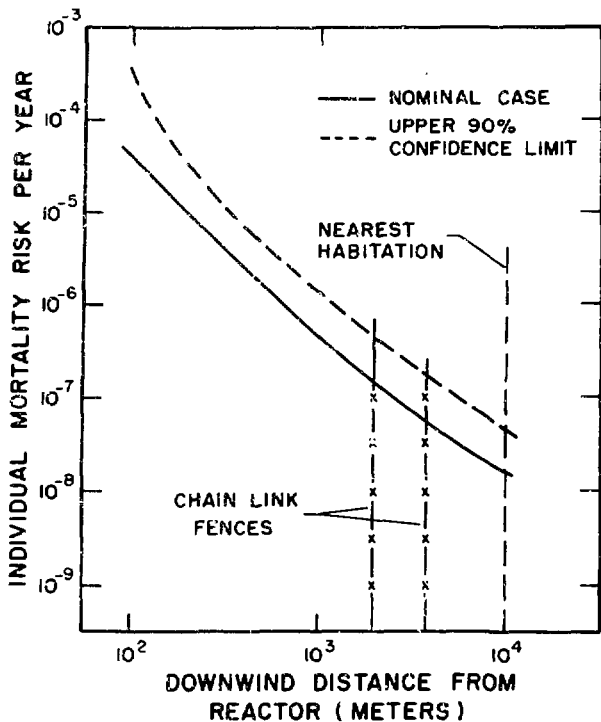
Fig. 5.
Yearly mortality risk vs distance (Pasquill condition
Type F, 1m/sec down-canyon wind).

uncontrolled structure. An aerial view of the area is shown in Fig. 7. The highest individual somatic risk to the population is about 5×10^{-10}/yr which, relative to the values of Sec. IV, is negligible. The risk added by the OWR would increase the chance of accidental death for an "average" person with "average" accident exposure by 0.0001%. The nonspecific life-shortening at the point of highest individual risk may be expressed as 25 sec per year of continuous exposure.

C. The Total Risk. The total risk, based upon a 30-yr reactor lifetime can be expressed as a detriment over all generations of 1.35×10^{-2} death. This figure is conservative because it also contains genetic deaths and the equivalent of nonspecific life-shortening. The total risks (30-yr reactor operation) are:

Somatic (acute and late)	5.1×10^{-5}
Nonspecific Life-Shortening	1.2×10^{-3}
Genetic	
First Generation	3×10^{-4}
Subsequent Generations	1.2×10^{-2}
Total	$\sim 1.4 \times 10^{-2}$

Based on 30 years of reactor operation, the total risk figure in the table above could also be expressed as 4.5×10^{-4} deaths per year. For comparison, a community this size ($\sim 13,000$)* would have about 2600 natural genetic deaths per generation, assuming natural mutation rates and genetic equilibrium. Also, on the basis of national accident statistics, there should be about 270 accidental deaths here in a 30-yr period.

VI. Conclusions

Our estimates of risk are pessimistic. The accident probability and fission-product release calculations were made conservatively, and the upper risk limit was estimated by assuming a continuous accident spectrum, i.e., an infinite number of discrete accidents. Further pessimism was introduced through use of linear consequence vs dose relationships, neglecting dose rate, biological repair, and threshold mechanisms. Note that the risk based upon the 90% upper confidence limit of the release-probability curve (see Figs. 3 through 5) is not appreciably greater than the nominal value. Previous work[1,2] showed that risk is not particularly sensitive to accident probability.

It is interesting that our accident source term (fission-product release vs accident probability curve, Fig. 2) is almost the same as that found in Refs. 1 and 2 for a 1000-MWe (3200-MWth) pressurized water reactor (PWR) and that the integrated source terms are almost identical. A couple of inferences could be made from this. One is that the source terms for most thermal reactors as presently designed and sited might be quite similar. A second is that this similarity may give a very crude measure of the effectiveness of some of the PWR safeguards. Namely, the PWR containment and atmospheric cooling and spray systems may account for an effective power reduction from 3200 to 8 MWth, a factor of 400. This statement must be viewed with extreme caution because there are many other basic differences in design between a PWR and a tank-type research reactor. For a given design, this approach might enable evaluation of specific safeguard systems in terms of equivalent power reduction. Another conclusion is that methods like this seem to be consistent in their assessment of reactor risk and provide the sort of numerical result that one would expect.

Finally, from this study, it appears that the indefinite operation of the Omega West Reactor at a power of 8 MWth presents no undue risk to the community of Los Alamos.
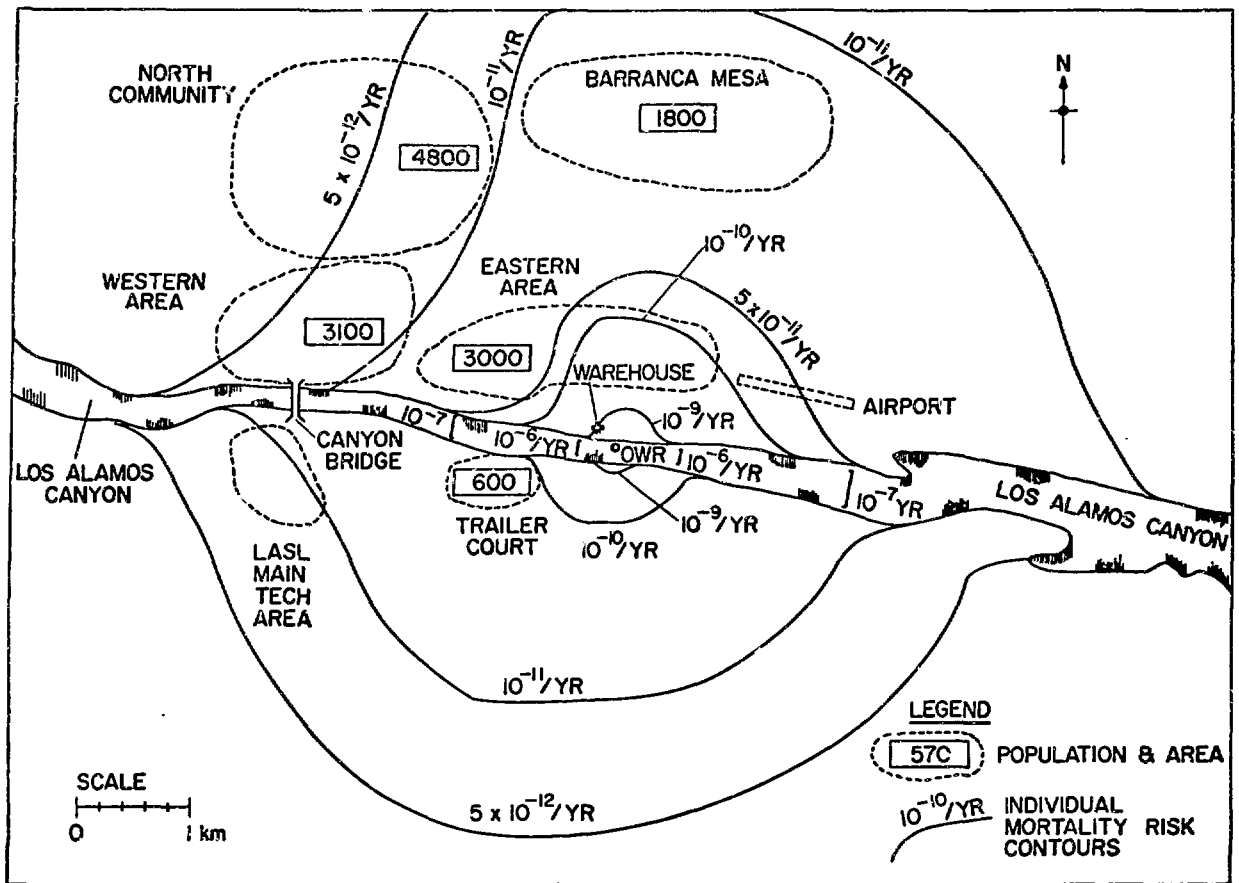

Fig. 6.
Individual mortality risk contours superimposed on plan of Los Alamos, New Mexico.

Notes on the Method. Two objections to analyses such as this are the difficulty in identification of all accidents and accident processes, and the problem of finding good reliability data for reactor systems and components.

First, we feel that a risk estimate based upon a continuous accident spectrum overestimates the risk that would be added by accidents that were overlooked or by interconnected faults. The sample of accidents used to establish this continuum included all those that could be identified and, while it is not a random sample, neither is it a biased sample.

Second, although accurate reliability data are scarce, it is not difficult to obtain conservative upper limits on failure rates from operating history and test data. The results show that risk levels based on these data are not even marginally high and, indeed, risk levels are not particularly sensitive to accident probabilities. This implies that conservative reliability estimates may be sufficient for risk analyses, so that precise reliability data are not necessary.

References

1. Harry J. Otway, "The Application of Risk Allocation to Reactor Siting and Design," Los Alamos Scientific Laboratory report LA-4316 (May 1970).

2. Harry J. Otway and Robert C. Erdmann, "Reactor Siting and Design from a Risk Viewpoint," Nucl. Eng. Design 12 (1970), in press.

3. *Accident Facts,* 1968 Ed., National Safety Council, Chicago, Illinois, 1968.

Fig. 7.

Aerial view (looking east) of Pajarito Plateau, showing OWR Site under arrow, Los Alamos townsite at left and center, and laboratory areas at right.

4. Harry J. Otway and Robert C. Erdmann, "Leukemia and Thyroid Carcinoma: A Comparison of the Late Mortality Risks from Reactor Accidents," Submitted to Nuclear Safety in June 1969. Scheduled for Volume 11, September-October 1970.

5. Samuel Glasstone, *The Effects of Nuclear Weapons*, Rev. Ed., U. S. Atomic Energy Commission, Washington, 1962.

6. G. Failla and P. McClement, "The Shortening of Life by Chronic Whole-Body Irradiation," Am. J. Roentgenol. Radium Therapy Nucl. Med. 78, 946 (1957).

7. W. L. Russell, "Shortening of Life in the Offspring of Male Mice Exposed to Neutron Radiation for an Atomic Bomb," Proc. Nat. Acad. Sci. U. S. 43, 324 (1957).

8. R. F. Kallman and H. I. Kohn, "Life-Shortening by Whole- and Partial-Body γ-Irradiation in Mice," Science 128, 301 (1958).

9. P. Alexander and O. Connell, "Shortening of the Life Span of Mice by Irradiation with X-Rays and Treatment with Radio-mimetic Chemicals," Radiation Res. 12, 38 (1960).

10. J. B. Storer, B. S. Roberts, I. V. Boone, and P. S. Harris, "Relative Effectiveness of Neutrons for Production of Delayed Biological Effects. II. Effect of Single Doses of Neutrons from an Atomic Weapon on Life Span of Mice," Radiation Res. 8, 71 (1958).

11. E. Lorenz, L. O. Jacobson, W. E. Heston, M. Shimkin, A. B. Eschenbrenner, M. K. Deringer, J. Doniger, and R. Schweisthal, Chapter 3 in "Effects of Long-Continued Total-Body Gamma Irradiation on Mice, Guinea Pigs, and Rabbits. II. Effects on Life Span, Weight, Blood *Ficture*, and Carcinogenesis and the Role of the Intensity of Radiation," *Biological Effects of External X and Gamma Radiation*, R. E. Zirkle, Ed., Part I, McGraw-Hill, New York, 1954, p. 24.

12. M. A. Blair, "Data Pertaining to Shortening of Life Span by Ionizing Radiation," University of Rochester report UR-442 (May 1956).

13. R. Seltzer and P. E. Sartwell, "The Influence of Occupational Exposure to Radiation on the Mortality of American Radiologists and Other Medical Specialists," Am J. Epidemiology 81, 2 (1965).

14. W. M. Court-Brown and R. Doll, "Expectation of Life and Mortality from Cancer among British Radiologists," Brit. Med. J. 2, 181 (1958).

15. S. Jablon, M. Ishida, and M. Yamasaki, "Studies of the Mortality of A-Bomb Survivors. 3. Description of the Sample and Mortality, 1950-1960," Radiation Rs. 25, 25 (1965).

16. W. L. Russell, "The Effect of Radiation Dose Rate and Fractionation on Mutation in Mice," in *Repair from Genetic Radiation Damage and Differential Radiosensitivity in Germ Cells*, F. H. Sobels, Ed., Macmillan, New York, 1963, p. 205.

17. M. F. Lyon and T. M. Morris, "Mutation Rates at a New Set of Specific Loci in the Mouse," Genetics Res. 7, 12 (1966).

18. M. F. Lyon, R. J. S. Phillips, and A. G. Searle, "The Overall Rates of Dominant and Recessive Lethal and Visible Mutation Induced by Spermatogonial X-Irradiation of Mice," Genetics Res. 5, 448 (1964).

19. K. G. Luning, "Studies of Irradiated Mouse Populations. III. Accumulation of Recessive Lethals," Mutation Res. 1, 86 (1964).

20. R. J. S. Phillips, "A Comparison of Mutation Induced by Acute X- and Chronic Gamma Irradiation in Mice," Brit. J. Radiol. 34, 261 (1961).

21. T. Sugahara, "Genetic Effects of Chronic Irradiation Given to Mice through Three Successive Generations," Genetics 50, 1143 (1964).

22. J. V. Neel, and W. J. Schull, *The Effect of Exposure to the Atomic Bombs on Pregnancy Termination in Hiroshima and Nagasaki*, Publication 461, Natl. Acad. Sci., Natl. Res. Council, Washington, 1956.

23. *The Evaluation of Risks from Radiation*, International Commission on Radiological Protection Publication 8, Pergamon Press, New York, 1966.

24. Report of the United Nations Scientific Committee on the Effects of Atomic Radiation, General Assembly Official Records: Twenty-First Session, Suppl. 14 (A/6314), United Nations, New York, 1966.

25. J. F. Crow, "The Estimation of Spontaneous and Radiation-Induced Mutation Rates in Man," Eugenics Quart. 3, 201 (1956).

APPENDIX A

THE OMEGA WEST REACTOR*

1. Introduction

The Omega West Reactor (OWR) is a thermal, heterogeneous, tank-type research reactor operated by the Los Alamos Scientific Laboratory (LASL). It provides sample irradiations, a source for external neutron and gamma-ray beam experiments, and facilities for irradiation of instrumented capsules.

The OWR was originally operated at a power level of 5.0 MW. In 1967, after 9 yr of operation, the power level was increased to 8.0 MW. The OWR normally operates on a 24-h/day, 5-day/week schedule.

2. Reactor Description

The OWR uses an assembly of material testing reactor (MTR)-type fuel elements supported inside a stainless steel tank. The core support structure and grid plate

are aluminum. Light water circulated downward through the core at 3500 gal/min serves as moderator and coolant. The reactor is controlled by eight blade-type poison rods. The reactor tank is covered with a stainless steel lid that supports the control-rod drive mechanisms and also contains two large hatches for access to the core. An irregularly octagonal biological shield of heavy concrete surrounds the tank and thermal column. Experimental ports open on all shield faces; a large thermal-column door opens on the east side. Instrumentation ports are in a recess at the bottom of the south face and extend underneath the core.

Figure A-1 is a cutaway view of the reactor.

(a) *Reactor Core.* The reactor core is a 4 by 9 array of fuel elements and experiment or sample elements supported vertically in the aluminum grid plate. Eight borated stainless steel control blades move in slots between fuel elements. A beryllium reflector is on the west face of the core, and a lead gamma shield on the east face; the north and south faces are water reflected.

(1) *Fuel Elements.* The metal fuel elements are of the type developed originally for the MTR. Each contains
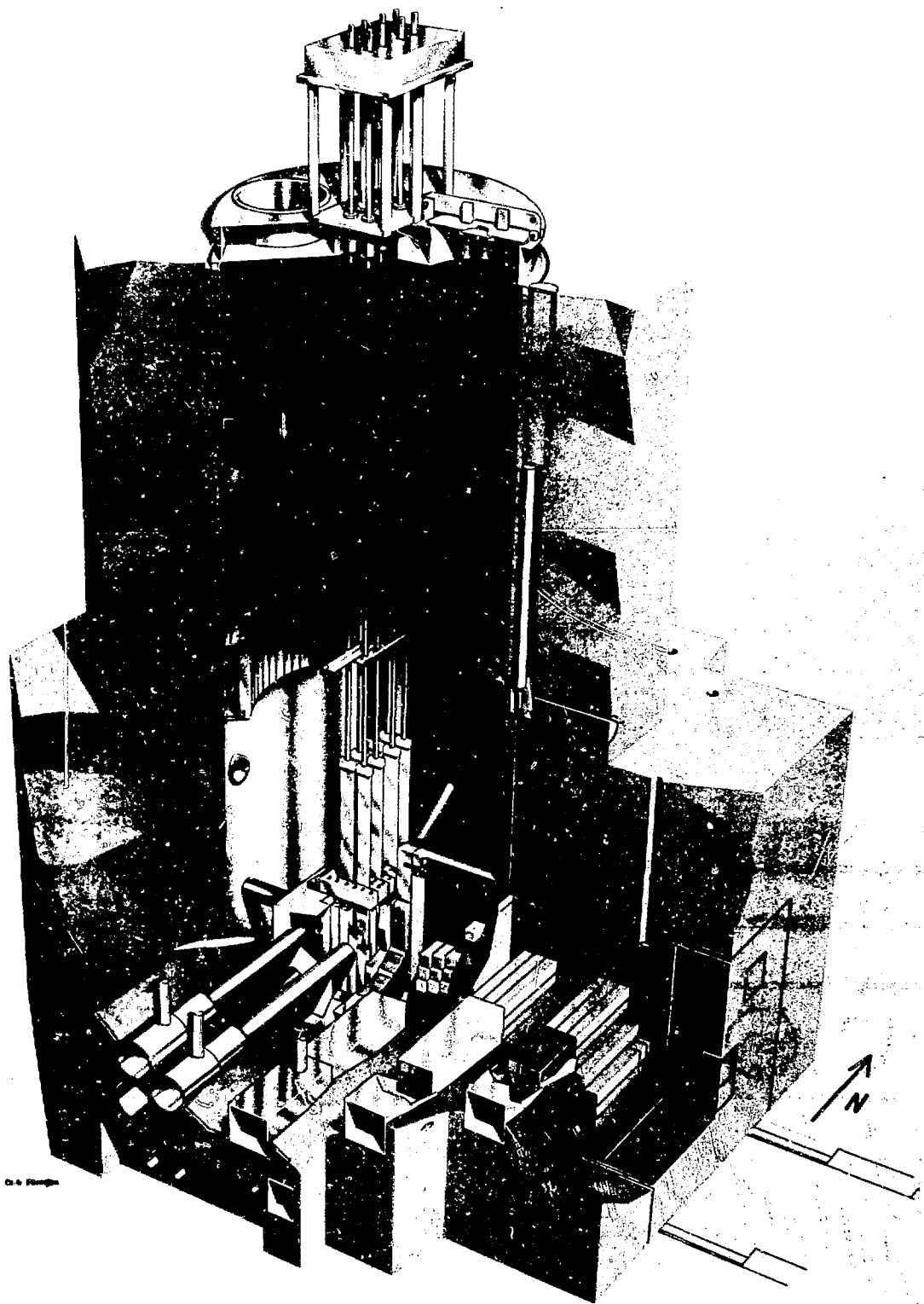

Fig. A-1
Cutaway view of OWR.

18 curved fuel plates, 60 mils thick, mounted 117 mils apart in heavy aluminum side plates. Each fuel plate is a sheet of uranium-aluminum alloy sandwiched and hot-rolled between two 20-mil-thick sheets of pure aluminum. The ^{235}U-bearing section of the elements is 24 in. long. A cylindrical end box welded to each end of the element positions it in the grid plate and permits water flow between fuel plates. Each fuel element contains 220 g of ^{235}U.

(2) Core Loading. The typical fuel loading is a 4 by 9 array containing 31 fuel elements and five positions for use as experimental and irradiation facilities. Figure A-2 shows this loading arrangement.

The fuel elements each initially contain 220 g of ^{235}U; however, the elements in a given core loading range from 0 to 33% in burnup, with the core containing an average of ~ 5.9 kg of residual ^{235}U. In a normal cycle,

four spent elements are replaced with new elements every 6 weeks to compensate for burnup. New elements are introduced at the ends of the core and shifted to progress toward the center during subsequent reloadings. This pattern tends to flatten the flux distribution.

(3) Control Rods. The reactor is controlled by eight independently movable stainless steel control rod blades, containing 1.2 wt% natural boron. The rods move in slots between fuel elements and are located in the core array as shown in Fig. A-2. Stainless steel extension rods attached to the top of the control rods extend upward through bearing holes in the two support bridges across the reactor tank (Fig. A-1). Just above the upper bridge, the extension rods become discontinuous through an armature and electromagnet assembly. In case of a scram or power failure, the magnetic coupling releases the rods which fall under gravity to the down position. Above the
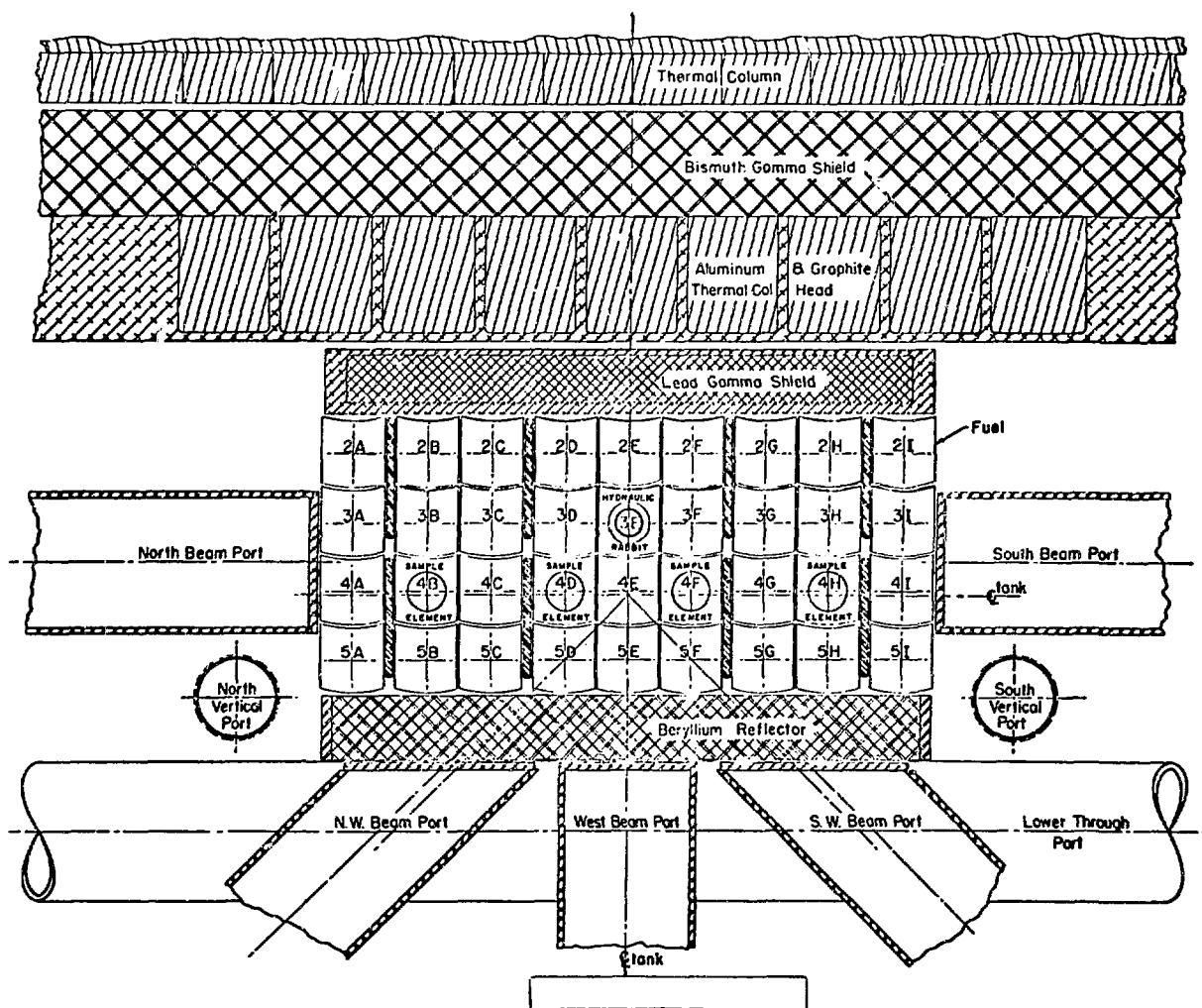

Fig. A-2
OWR core layout.

magnet assembly, the rods pass through chevron seals in the reactor tank lid. Just above the lid, they are coupled through a rack and pinion to the drive mechanism, consisting of a reduction gear box and drive motor. Motor controls are interlocked so that only one rod can be raised at a time. The control rods are routinely replaced after 90,000 MW h of operation, although this exposure does not adversely affect their mechanical properties.

(b) Reactor Tank. The OWR reactor tank is a stainless steel cylinder, 8 ft in diameter and about 24 ft high with 1/4-in.-thick walls and 3/8-in.-thick bottom plate. The lid is bolted to the top flange of the tank and sealed with an O-ring. The lid contains two 28.5-in.-diam hatches for access to the interior. Heavy glass viewing windows in the hatches allow observation of the core and tank interior during reactor operation. The tank contains the following penetrations.

(1) Coolant Inlet and Outlet Coolant Lines. The 12-in.-diam coolant inlet line enters the reactor foundation ~ 6 ft below the tank bottom and extends upward through the concrete shield to the tank inlet 49 in. above core centerline. Water flow through the core is downward through the fuel elements into the base structure and out the 12-in.-diam exit pipe through the tank bottom. From there, the exit line passes up along the reactor tank, inside the concrete shield, to 49 in. above core centerline before making a U bend and going back below floor level into the large delay line. At the top of the U bend in the exit pipe, a short 12-in.-diam pipe reenters the reactor tank through a "flapper" valve. A more complete discussion of this system is given in Sec. 4(a)(2) below.

(2) Five Beam Ports. Five 6-in.-diam horizontal beam ports enter the reactor tank at the core centerline.

(3) Two Horizontal Through Ports. The 6-in.-diam through ports pass alongside the core within a few inches of the west face and extend through the shielding at each end.

(4) Inclined Port. The inclined port is a 4-in.-diam tube that angles 30° from the horizontal down to just above the core centerline.

(5) Instrument Ports. Five 4-in.-diam instrument ports extend through the tank wall to positions under the core. These ports house ion chambers.

(6) Tank Drain Line. The 1-in.-diam stainless steel drain line enters 15½ in. above the tank bottom, bends 90°, and extends to 1 in. above the bottom where it terminates in a gate valve.

(7) Thermal Column. The 6-ft-diam stainless steel thermal-column liner is welded into the reactor tank at floor level and extends into the tank to a position adjacent to the core. An aluminum head is bolted to the liner flange; a stainless steel O-ring between the head and flange serves as a watertight seal.

(c) Reactor Shielding. Biological shielding above the reactor is provided by the 17 ft of water above the fuel. A heavy-concrete shield surrounds the tank and thermal column. This shield is 5 ft thick to a height of 11 ft above the reactor room floor and is at least 3 ft thick above that.

3. Reactor Control and Instrumentation

(a) Reactivity. Maximum allowable excess reactivity for the OWR is 13%. Present operational requirements call for an available excess reactivity of 8%, utilized as follows.

Equilibrium xenon	3.5
Xenon override	0.7
Fuel burnup	2.8
Samarium and stable fission products	0.3
Temperature coefficient	0.2
Experiments	0.5
TOTAL	**8.0%**

The eight boron-stainless control blades serve as both safety and shim rods, with the four center rods being used as regulating rods at a slower speed for automatic control.

The control-rod drive speeds give reactivity insertion rates compatible with both safety and operational requirements. The available reactivity insertion rates are:

Average	
manual	4.5×10^{-4} $\Delta k/k$ sec,
automatic	1.6×10^{-5}
Maximum	
manual	1.2×10^{-3} $\Delta k/k$ sec,
automatic	2.7×10^{-5}

The automatic rates are for the four center rods moved as a gang; the manual rates are for movement of one rod at a time.

The instrumentation and safety systems are simple and reliable. For reactor startup, check lists are used instead of chains of permissive interlocks, thereby eliminating much complication without significantly affecting safety. Only one type of automatic safety action, the full scram, is provided; no automatic setbacks, rundowns, or reverses are used. All scram channels are independent, and only one signal is required to initiate a scram.

(1) Safety System. Current to the rod-lifting magnets is supplied by a fail-safe electronic current source. The magnet-current control chassis is an electronic trip

and cuts off the dc supply to the magnets upon loss of the 150-V scram-bus voltage. A superimposed ac component helps reduce the rod breakaway time. Scrams are triggered by breaking the scram-bus line with relays. The safety circuit response time averages 63 msec from the input of a scram impluse to the instant the rods break away from the magnets.

Any of the following conditions will initiate a reactor scram.

> High power level, channel 1
> High power level, channel 2
> High power level, channel 3
> Short period
> Loss of coolant flow
> Loss of pump power
> High coolant exit temperature
> Fail-safe voltage scrams (2)
> Experiment scrams (as needed)
> Manual scram

(2) Neutron Instrumentation. Six neutron monitoring channels provide the necessary level and period coverage from startup to operating power. These channels are as follows.

Log Count-Rate Channel. This channel provides low-level coverage during core loading and reactor startup. Range coverage for the count-rate channel is from about 0.1 W to 8kW.

Log N-Period Channel. This is a conventional log level and period channel providing coverage from the 8-W to 24-MW level. Overlap between this channel and the log count-rate channel is at least three decades.

Power-Level Safety Channels. These three linear level channels provide power-level indication in the power range and input to three power-level scram circuits.

Integrator Channel. This channel provides an audible signal, proportional to reactor power, for routine operation at the design power level.

Differential Level Channel. This channel provides a suppressed magnified level signal, and its principal use is to detect small reactivity changes.

Automatic Power-Level Control. The automatic control system uses the output of one of the linear channels and holds the reactor power constant. The system is a discontinuous, or on-off, type of servo control and is used only at constant power levels. A "servo-fault" circuit removes the system from servo control and prevents rod withdrawal if the error signal calls for too large an increase in power level.

(3) Annunciator System. A host of annunciators

provides visual and audible alarms of off-standard operating conditions and those that may be approaching potentially dangerous limits.

(4) Electrical Power System. The OWR site is serviced by an overhead 13.2-kV electric power line. Power from this line is divided into a 750-kVA regular service and a 100-kVA special service for reactor and experiment instrumentation. In case of a power failure, an emergency gasoline-powered generator is available to power essential equipment, such as radiation monitors and public address system. It does not power the OWR main circulating pump. The generator is a three-phase, 110/208-V, 25-kW, 31-kVA set that must be manually started and transferred.

4. Reactor Cooling System

The reactor is cooled by demineralized light water circulated downward through the core at 3500 gal/min. Figure A-3 shows the principal reactor cooling system. After it leaves the core, the cooling water passes through a delay line, a surge tank, a pump, and a cooling tower before being returned to the reactor tank. Water purity is maintained by bypassing a small stream through a deionizer and filter system. Two auxiliary pumps provide emergency flows to prevent freezing in case of loss of the main pump in winter and for cleanup in case of radioactive contamination of the water system.

(a) Primary Cooling Loop. *(1) Main Circulating Pump.* The 3500-gal/min flow through the primary loop is produced by a double-suction, stainless steel, 8-in. pump driven by a 100-hp electric motor and provides the necessary core cooling, plus a margin of safety against boiling in the core. The main flow from the pump to the 8-MW cooling tower and from the tower back to the reactor is through 10- and 12-in.-diam stainless steel piping. A servo-operated butterfly valve in a 10-in. bypass line around the tower heat exchangers allows the reactor inlet cooling water to be kept at a constant temperature, usually 40°C. From the heat exchangers, the water returns to the reactor tank through an underground, 12-in. stainless steel pipe. An orifice plate in this line provides a flow signal to the control room from a pneumatic differential-pressure transducer.

(2) Flapper Valve. Water flow through the core is downward through the fuel elements into the base structure and out the 12-in.-diam exit pipe through the bottom of the tank. From there, the exit line passes upward alongside the reactor tank, inside the concrete shield, to 49 in. above the core centerline before making a U bend and going back below floor level into the large delay line. At the top of the U bend in the exit pipe, a short 12-in. pipe reenters the reactor tank. This entrance is covered by a flapper valve. During normal cooling flow, the flapper valve is kept closed by the pressure drop across the core;
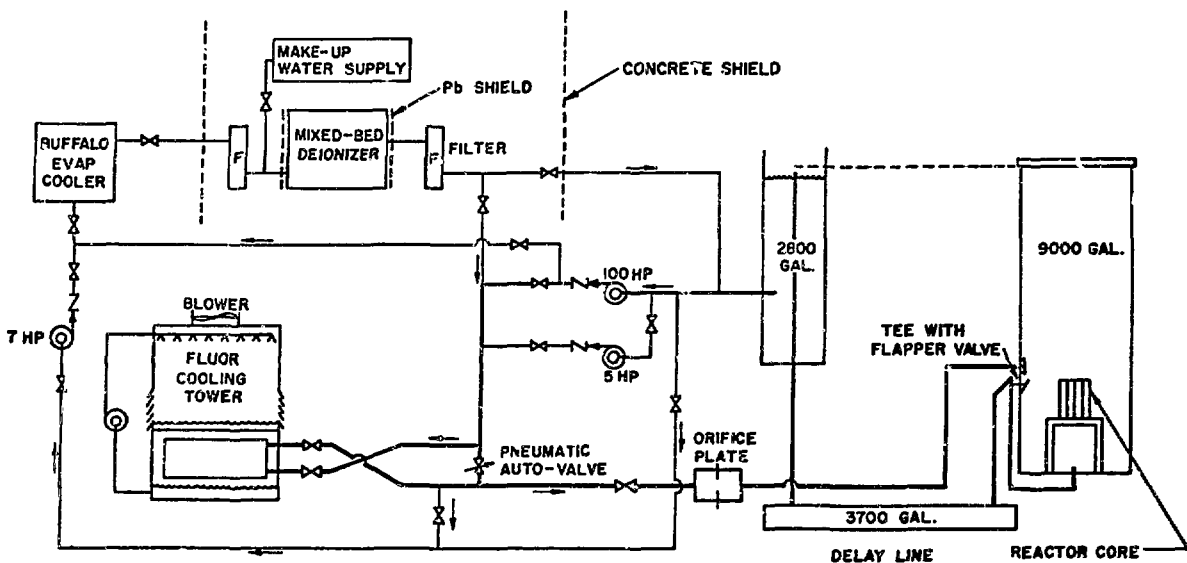
Fig. A-3.
Principal reactor cooling-system flows.

when flow is lost, the valve opens under its own weight.

The flapper valve serves two functions: it provides a path for convective cooling to help remove afterheat and to allow for operation at power levels up to 400 W, and it serves as an antisiphon device to prevent draining of water from the reactor tank to below the level of the flapper valve in case of a major break in the water lines.

(3) Delay Line. The return cooling-water line from the reactor to the surge tank contains a 104-ft-long enlarged section of 30-in.-diam stainless steel pipe which serves as a delay line or holdup tank. The resulting delay of ~ 1 min allows the ^{16}N activity to decay to a safe level before the water enters the surge tank. The top of the delay line is at least 6 ft underground.

(4) Surge Tank. From the delay line, the cooling water enters an aboveground surge tank, 19 ft high and 5 ft in diam, with a total capacity of 2800 gal. Water enters at the bottom through a standpipe that extends 17 ft into the tank. This standpipe fixes the water level in the reactor tank, when the pump is off and the hatches are open, at a few inches below the top of the hatch openings. The surge tank serves several additional purposes: it is an expansion volume to allow for water temperature changes, it provides the suction head for the main circulating pump, and it is a degassing surface for the water.

The water level in the surge tank is normally 16 to 18 ft. In the top of the tank is a two-way valve that allows the air space above the water to be vented to the atmosphere or the air exhaust stack. The tank is usually vented directly to the atmosphere because the quantities of H_2,

O_2, and radioactive gases evolved are small (less than 0.2 ft^3/h). In case fuel-element rupture or experiment failure releases radioactivity into the cooling water, the vent valve can be switched to the stack line from the control panel. A radioiodine filter trap is installed in the stack line just downstream from the two-way valve before the line enters the main air exhaust system to the stack.

(b) Emergency Core Spray Systems. Because the OWR reactor tank has penetrations through its walls, a rupture or leak in one of these penetrations, resulting from a failure or accident, could lead to loss of coolant. To provide enough cooling water in the form of spray to prevent core melting, two spray systems are installed in the reactor tank. These independent systems are designed for maximum reliability of operation and practicable redundancy.

(1) Emergency Core Spray System No. 1. This system utilizes the city water supply from the 8-in. fire water main system and will deliver up to 100 gal/min flow through a spray nozzle manifold assembly installed directly above the reactor core. Heat transfer analyses indicate that the spray system flow capability is an order of magnitude greater than necessary to prevent melting damage to fuel-element cladding. Operation of this system is manual and on the decision of the operating crew. Figures A-4 and A-5 show the routing and valve layout. Function of this system is checked each week by an indirect procedure. The reactor coolant water backflow is verified by successively operating the isolation valves between the backflow preventer and the reactor. Then the
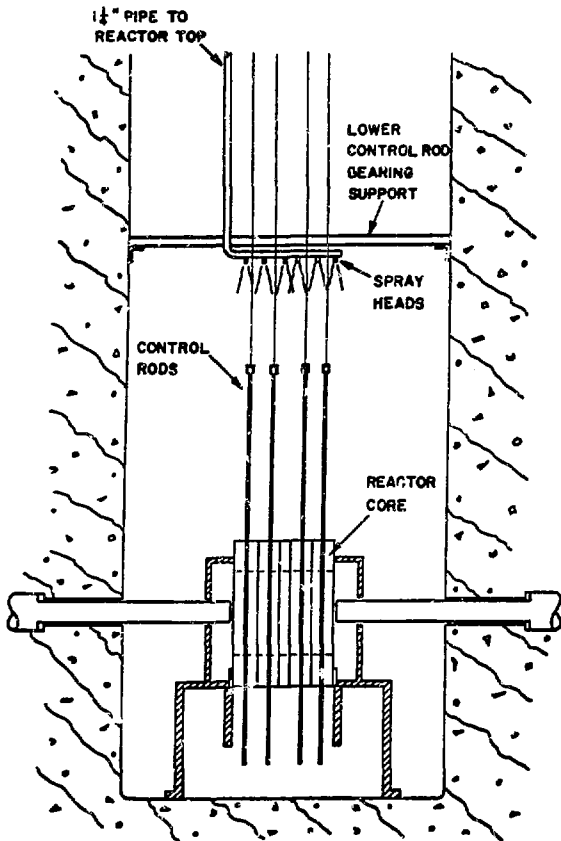
Fig. A-4.
Emergency core-spray system No. 1, showing location of spray nozzles directly above core.
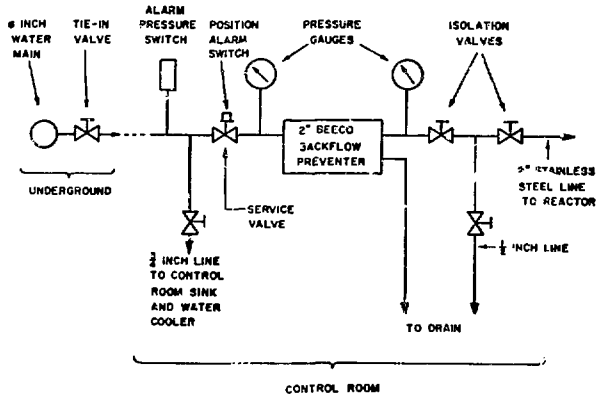
Fig. A-5.
Valve arrangement for core-spray system No. 1.

fire-main water flow up to the reactor isolation valve assembly is checked, thus verifying the total unobstructed flow path. The spray system shutoff valve arrangement is shown in Fig. A-5.

(2) Emergency Core Spray System No. 2. This system has a secure source of pure reactor-system water, is not dependent on the reactor tank lid structure for support, is fully automatic, and is checked in a direct functional test each week. The system utilizes a 3-hp, electrically driven centrifugal pump to deliver cooling spray to the core at about 18 gal/min. The pump draws water from the 1-in. drain line at the bottom of the 30-in. delay line and delivers it through two, 15-degree, solid cone, 1/2-in. spray nozzles mounted in a recess in the tank wall below the lid. A flow meter in the discharge line measures the flow rate. Because the capacity of the 30-in. delay line is about 3700 gal, there is ample water to maintain the spray at 18 gal/min for about 3½ h. The angle and direction of the two nozzles were set for optimal spray coverage on the core during full-scale mock-up tests. Fig. A-6 shows the location of the spray nozzles in the reactor tank. This spray system is automatically actuated by liquid-level sensors that measure the water level in the reactor tank and provide audible and visual annunciator alarms at the reactor console.

Fig. A-6.
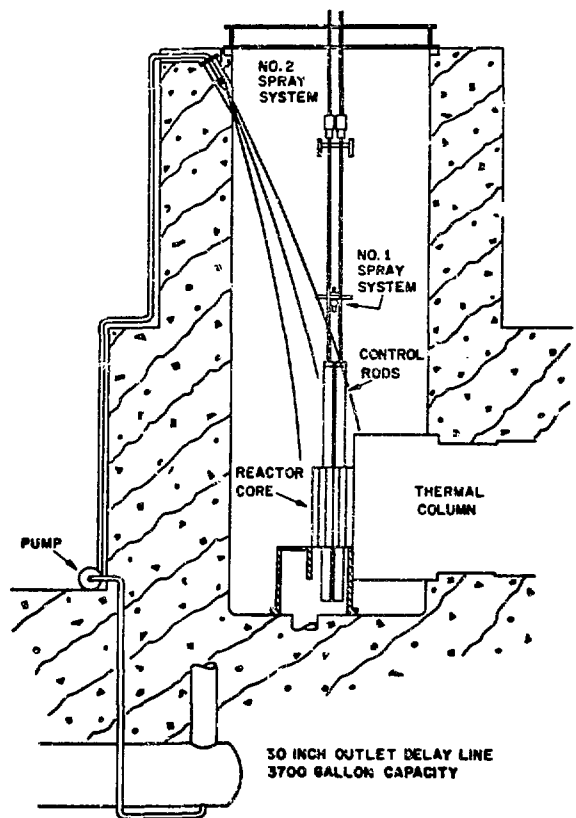Emergency core-spray system No. 2, showing locations of delay-line reservoir and spray nozzles in recess below tank lid.

5. Site and Facilities

(a) Site. *(1) Location.* The OWR site, officially designated TA-2, is commonly known as Omega Site. It is in Los Alamos County in northern New Mexico, approximately 24 miles northwest of Santa Fe (see Fig. A-7). Developments within Los Alamos County include Los Alamos townsite, Barranca Mesa and White Rock residential areas, and the LASL technical areas. The location of TA-2 with respect to these is shown in Fig. A-8 along with the local area populations.

(2) Geography. Los Alamos County is situated on the Pajarito Plateau, a region 5 to 6 miles wide and ~ 7300 ft above sea level, between the 10,500-ft-high Jemez Mountains to the west and the 5500-ft-high Rio Grande Valley to the east. The plateau is cut by many deep canyons running generally eastward from the mountains to the river. The OWR site is in the bottom of such a canyon, known as Los Alamos Canyon.

Figure A-9 is a map of the lower part of Los Alamos Canyon. The distance from TA-2 to State Road 4 at the lower end of the canyon is 4 miles. This part of the canyon is unoccupied: fences with locked gates cross the canyon 1.2 and 2.7 miles below the reactor site. The entire canyon from above the reactor site to State Road 4 is under the control of the AEC. A profile of Los Alamos Canyon at TA-2 is shown in Fig. A-10. At this point, the canyon is approximately 1350 ft wide at the top, and 350 ft deep. The sides are exceedingly rough and rocky and are partially covered by pine trees, particularly the south side. The bottom of the canyon is also wooded and fairly flat for a width of 200 ft. Through this area passes a small stream, normally dry except for short periods during spring runoff and summer thunderstorms.

The region immediately surrounding the reactor site is shown in Fig. A-11. Approximately one-third mile up the canyon west of TA-2 is TA-41 (W Site), a LASL technical area used by weapons engineering groups. The main access road to TA-2 approaches the site from the west along the canyon floor, passing just south of TA-41. This road ends at TA-2, although a trail passable to four-wheel-drive vehicles continues down the canyon to State Road 4.

(b) Reactor Building and Other Facilities. The main building at the OWR Site is a two-story structure of concrete blocks and wood. The OWR is located in a room 55 by 45 by 24 ft high at the west end of this building. The building walls, except the east one, are of 8-in. concrete building blocks. The east wall is one side of a 5-ft-thick earth fill contained in concrete; the other parts of the building are shielded by this fill. Neither the building nor the reactor itself affords any containment of the reactor system above the maximum design pressure of the tank lid.

Other buildings include one for general storage and another for storage of slightly radioactive equipment. Another houses the main circulating pump, auxiliary pumps, and two mixed-bed deionizers.

Other facilities include storage for highly radiative material and underground storage tanks for liquid waste.
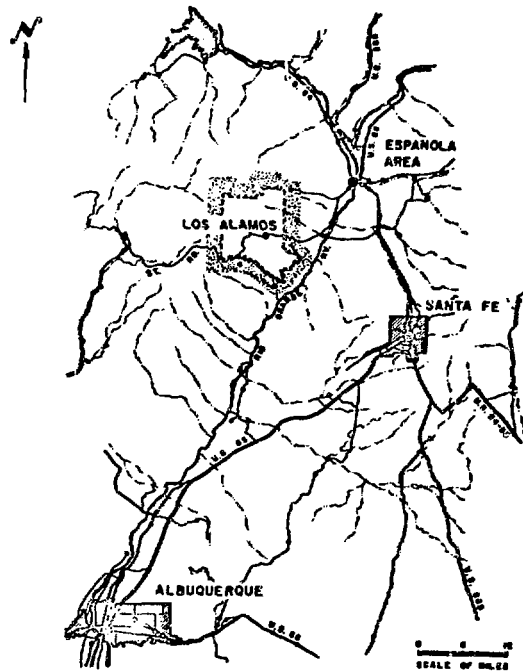
Fig. A-7.
Los Alamos and vicinity.

NORTH

BARRANCA
MESA [1500]

RESIDENTIAL
AREA [8400]

[2550]

[110] TA-2 [30] TA-21 [85] TA-53 TA-28

TA-43 TA-41

TA-3 [2500] TA-46 [60] TRAILER
COURT [370]

TA-8 [10] TA-3 [40] TA-42 TA-35 [130]

TA-9 [35] TA-22 [70] TA-40 [30] TA-50 [35] TA-52 [40] TA-5

TA-46 [150]

TA-16 [280] TA-4 TA-51 [10] TA-54

TA-11 [5] TA-15 [100] TA-18 [55]

TA-28 TA-37 [1] TA-36 [23]

S.P.R.
CAMP [30] TA-49 [10]

WHITE ROCK
[3050]

TA-39
[35]

BANDELIER
[40] TA-33
[45]

NOTE

[52] DENOTES POPULATION

1000 0 2000 4000 6000 8000 10000

SCALE IN FEET

Fig. A-8.
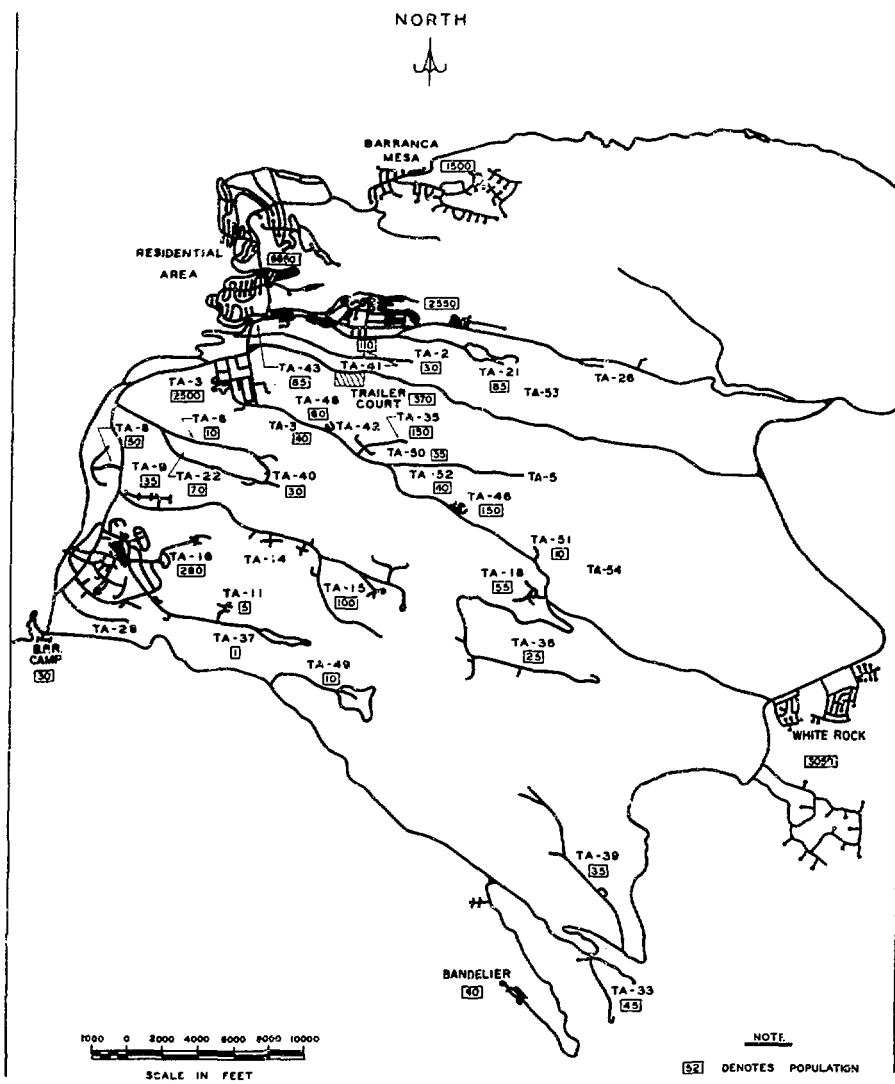*Los Alamos townsite and laboratory technical areas. Boxes show local area populations.*
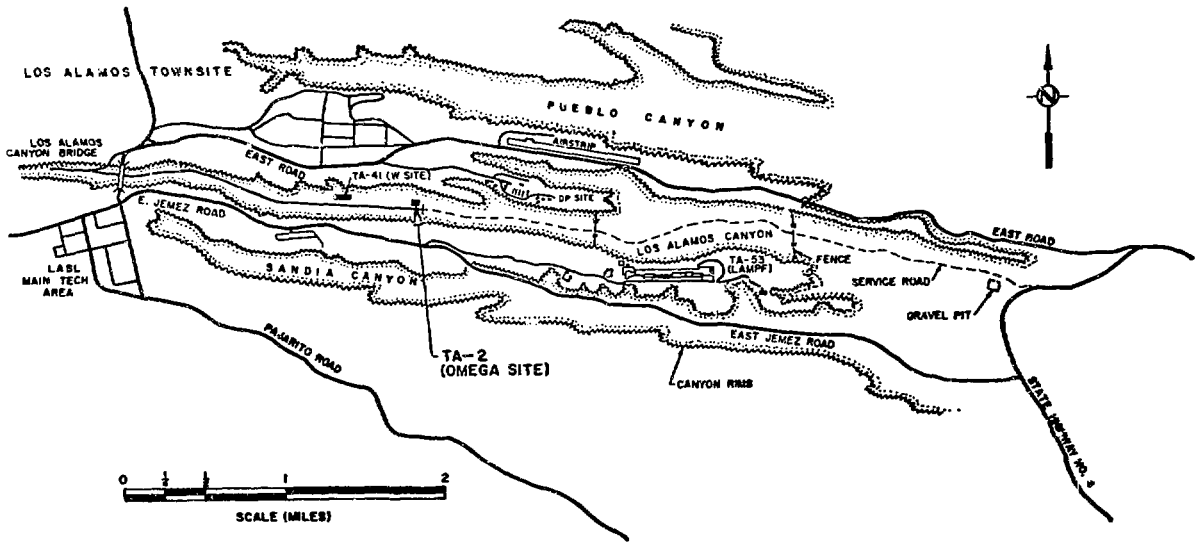
18

Fig. A-9.
Lower end of Los Alamos Canyon.

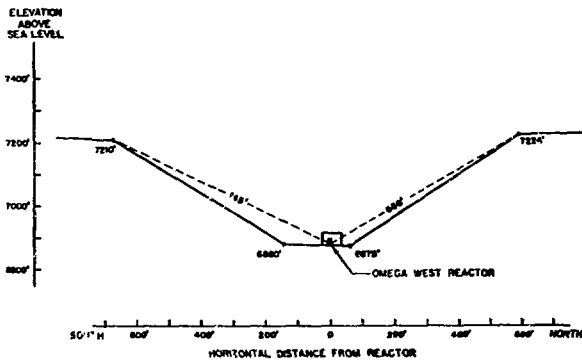*Fig. A-10.*
*Profile of Los Alamos Canyon at OWR Site. Slopes
are shown straight, but actually consist of several
vertical steps and shelves.*

Fig. A-11.
Relative locations of OWR Site and W Site. Land tracts above the canyon rim to the north are described in the text.

APPENDIX B

PROBABILITY AND STATISTICS

1. Probability of an Accident

For accident chain calculations, we assume that the probability of an individual component's failing is either independent or completely dependent. If failure of component A is completely dependent upon component B, then when B fails the $P[A$ fails $| B$ fails$] = 1$.

All components, say C, D, E, and F, of a system must fail for the accident to occur. Thus if we use the notation $P[C]$ to mean the probability of C failing, we can write the chain of accident 1 as

$$P[1] = P[C] \ P[D|C] \ P[E|C,D] \ P[F|C, D, E] \quad .$$

However, the above assumption of independence gives

$$P[1] = P[C] \ P[D] \ P[E] \ P[F] \quad . \qquad (B-1)$$

In some cases a component, say B, is made up of two or more subcomponents, say B_1 and B_2, failure of either of which causes B to fail. In this case the probability of B failing is

$$P[B] = P[B_1] + P[B_2] - P[B_1] \ P[B_2] \quad .$$

These probabilities were computed as explained in the next section when we saw k failures in a period of time, T. However, when we saw no failures during time T, we used the 90% upper confidence limit (Eq. (3) in text) as a conservative estimate for the failure rate.

The 90% upper confidence limit was computed for each individual link of the probability chain, and the product was then taken to give a conservative 90% upper confidence limit for each accident. Take, for example, Eq. (B-1); the upper confidence limit was computed for $P[C]$, $P[D]$, $P[E]$, and $P[F]$, and these values were multiplied together to give the 90% upper confidence limit for $P[1]$.

2. Estimation of Failure Rates

The assumption of a Poisson process with gamma-distributed waiting times and independent exponentially distributed inter-arrival times was used in estimation of the failure rates. The Poisson process assumes that the failures in a period of unit duration occur randomly at a mean rate, ν, per unit time. Thus, the main requirement to satisfy the above assumption is that the failures occur randomly in time at a constant rate. We assume that the reactor components are maintained and repaired as necessary and thus have negligible wear-out affect. This satisfies the assumptions of the Poisson process.

Let W_n be the waiting time until the nth event in a series of events occurring in the interval 0 to ∞ in accord with a Poisson process at a mean time to failure, ν. Then W_n is distributed as a gamma random variable with parameters n and ν; i.e.,[B 1]

$$f_{W_n}(t) = \nu e^{-\nu t} \ \frac{(\nu t)^{n-1}}{(n-1)} \qquad t > 0 \qquad (B-2)$$

$$= 0 \qquad t < 0 \quad .$$

If we made the transformation $Y = 2 \nu W_n$, we have

$$f_Y (t) = \frac{1}{2^n (n-1)!} \ t^{n-1} e^{-t/2} \qquad t > 0$$

$$= 0 \qquad t < 0 \quad ,$$

which is a chi-square distribution with $2n$ degrees of freedom. Therefore we can use the chi-square tables to find the $1 - \alpha$ confidence interval,[B 2] where

$$1 - \alpha = P\left[\chi_{\alpha/2}^2 (2n) \leqslant Y \leqslant \chi_{1-\alpha/2}^2 (2n) \right] \quad ,$$

$$= P\left[\chi_{\alpha/2}^2 (2n) \leqslant 2 \nu W_n \leqslant \chi_{1-\alpha/2}^2 (2n) \right] \quad ,$$

$$= P\left[\frac{\chi_{\alpha/2}^2}{2W_n} \leqslant \nu \leqslant \frac{\chi_{1-\alpha}^2 (2n)}{2W_n} \right] \quad .$$

The difficulty with this confidence interval is that W_n is the waiting time until the nth event occurs but usually the data are in the form of the number of failures, n, that occur in a fixed time, T. To place a confidence interval on ν using this information, Epstein[B 3] suggests using

$$P\left[\frac{\chi_{\alpha/2}^2 (2n)}{2T} \leqslant \nu \leqslant \frac{\chi_{1-\alpha/2}^2 (2n+2)}{2T} \right] = 1 - \alpha \quad . \ (B-3)$$

This is very advantageous in putting an upper confidence limit on ν when no failures have been observed in time T and the lower $1 - \alpha$ confidence interval is

$$P\left[0 \leqslant \nu \leqslant \frac{\chi_{1-\alpha}^2 (2)}{2T} \right] = 1 - \alpha \quad .$$

Generally, we used only the upper confidence limits for all failure rates. The general formula used when n

failures are observed in time T is

$$P\left[0 < \nu < \frac{\chi^2_{1-\alpha}(2n+2)}{2T}\right] = 1 - \alpha \quad . \qquad (B\text{-}4)$$

Also, the α level was generally chosen equal to 0.10.

We have shown that a confidence interval can be placed upon ν, the mean time to failure, when the estimate $\nu = n/T$. However, we want a failure rate value that is the probability of a failure for a fixed period of time. From Eq. (B-1), we see that the distribution of the waiting time to the first failure is

$$f_{W_1}(x) = \nu e^{-\nu x} \qquad x > 0$$
$$= 0 \qquad x < 0 \quad ,$$

which is the exponential distribution. Thus the probability of a failure in a given period of time, or the failure rate, is

$$Q(t) = \int_0^t \nu e^{-\nu x}\, dx = 1 - e^{-\nu t} \quad . \qquad (B\text{-}5)$$

For $t > 100$, $Q(t) \cong \nu$.

One can also find a failure rate for the upper confidence limit by using Eq. (B-5) where

$$\nu = \frac{\chi^2_{1-\alpha}(2n+2)}{2T} \quad .$$

References

B1. Emanuel Parzen, *Stochastic Processes*, Holden-Day, Inc., San Francisco, 1962, p. 134.

B2. Igor Bazovsky, *Reliability Theory and Practice*, Prentice Hall, Englewood Cliffs, New Jersey, 1961, p. 235.

B3. B. Epstein, "Estimation from Life Test Data," IRE Trans. Reliability Quality Control RQC-9, (1960).

APPENDIX C

DISPERSION AND DOSE CALCULATIONS

1. Introduction

The calculted doses and risk estimates presented here are based on the operating conditions, meteorology, and accident analysis peculiar to the Omega West Reactor (OWR). The calculational procedure was, briefly, as follows. Atmospheric dispersion and ground deposition factors for a given meteorological condition were computed for several downwind distances. These factors were used to compute thyroid and whole-body doses for a "unit" source release to the atmosphere. The computed dose at a selected down-wind distance, together with the data on atmospheric release vs accident probability per year (Fig. 2 in text), were then combined to yield an integrated dose which, in turn, was converted to an individual mortality risk figure. These were repeated for other downwind distances, and the individual mortality risks vs distance were plotted. The entire cycle was then repeated for other meteorological conditions of interest. Because all exposure points were always assumed to be downwind from the source point, the risk estimates were modified to represent the available wind and weather distribution data at the reactor site. Finally, the "weather-corrected" risk estimates were used to infer lines of constant individual mortality risk on a map of the surrounding townsite (Fig. 6 in text).

2. Fission-Product Inventory

Many compilations of the fission-product inventory from ^{235}U thermal fission have been published,[C1] including the summation studies of Perkins and King[C2] and a later revision by Perkins.[C3] Perkins' summation was further updated by Koebberling et al.,[C4] who also incorporated their data in a computer code, the Lockheed Fission Product Inventory Code (FPIC). Fission-product inventories for the OWR were computed using the FPIC-U/Pu code,[C5] an expanded version of the FPIC code capable of computing inventories appropriate to ^{239}Pu fast fission. While the plutonium data were being added to the FPIC library, some changes were made, including the addition of ^{91}Y.

For the OWR risk analysis, fission-product inventories were computed for a reactor operating cyclically over a 48-week period at 8 MW. Forty-eight operating cycles were assumed, each consisting of a 2-day shutdown followed by 5-day operation at 8 MW. The assumed 48-week operating period does not take into account the OWR refueling schedule, by which four spent elements are replaced with new elements every 6 weeks. Further, the inventory per fuel element was assumed equal to the total inventory divided by the 31 fuel elements in the core. Results of these computations for the nuclides of interest are shown in Table C-I as are the thyroid dose conversion factors (rads/curie inhaled) for the iodine isotopes.[C6]

TABLE C-I

FISSION-PRODUCT INVENTORY AT ZERO SHUTDOWN TIME
(Curies/fuel element = total curies/31 fuel elements.)

Nuclide	Curies/8 MW	Curies/Fuel Element	Rads/Curie Inhaled
^{83m}Kr	3.53 x 10^4	1.14 x 10^3	
^{85m}Kr	8.99 x 10^4	2.90 x 10^3	
^{87}Kr	1.72 x 10^5	5.55 x 10^3	
^{88}Kr	2.43 x 10^5	7.84 x 10^3	
^{131}I	1.65 x 10^5	5.32 x 10^3	1.48 x 10^6
^{132}I	2.55 x 10^5	8.23 x 10^3	5.35 x 10^4
^{133}I	4.51 x 10^5	1.45 x 10^4	4.0 x 10^5
^{134}I	5.40 x 10^5	1.74 x 10^4	2.5 x 10^4
^{135}I	4.22 x 10^5	1.36 x 10^4	1.24 x 10^5
^{131m}Xe	1.32 x 10^3	4.26 x 10	
^{133m}Xe	9.08 x 10^3	2.93 x 10^2	
^{133}Xe	3.50 x 10^5	1.13 x 10^4	
^{135m}Xe	1.27 x 10^5	4.10 x 10^3	
^{135}Xe	4.36 x 10^5	1.41 x 10^4	
^{138}Xe	3.80 x 10^5	1.23 x 10^4	

3. Assumptions Made in the Calculations

The assumptions made in computing the doses and mortality risks are as follows.

(a) Meteorological conditions

(1) Cross canyon (N and S of reactor). Pasquill Type C with 5 m/sec wind speed.

(2) Down canyon (E of reactor). Pasquill Type F with 1 m/sec wind speed.

(3) Up canyon (W of reactor). Pasquill Type C with 1 m/sec wind speed.

These conditions are the same as those used in the 1969 status report on the OWR[C7] except that we used a cross-canyon wind speed of 5, rather than 10, m/sec.

(b) The radioactive leak is a continuous, ground-level, point source with a short release period.

(c) Iodine deposition velocity of 1 cm/sec. Radioactive cloud source strength corrected for ground deposition.

(d) For thyroid inhalation dose and whole-body dose from the radioactive cloud, fission-product decay was neglected. Doses were computed for exposure during entire period of cloud passage.

(e) Whole-body dose from ground deposition of iodines is for infinite exposure with radioactive decay taken into account, and exposure point 1 m above ground.

(f) If F is the core fraction assumed to have melted, (1.0 x F) of the total Xe-Kr inventory is released to the atmosphere.

(g) If F is the core fraction assumed to have melted, (0.5 x F) of the total iodine inventory is released to the reactor tank. If the core is covered by water, the release to the atmosphere is (0.05 x F = 0.5 x 0.1 x F). If fuel melting occurs after drainage of the reactor tank, the release to the atmosphere is (0.25 x F = 0.5 x 0.5 x F). Finally, if the iodines are released to the atmosphere through the stack filters, an additional attenuation of 0.01 (99% filter efficiency) is assumed.

4. Dose Calculations

For the dose calculations, the release of all iodines and noble gases from one fuel element was chosen as the "unit" source. In computing the doses from a postulated accident, the release fractions appropriate to the core fraction melted and the circumstances of the release (see (f) and (g) above) were applied to the normalized "per element" values. It was convenient to introduce two quantities, K_x and F_d, defined as follows:

K_x = dilution factor = $1/(\pi \bar{u} \, \sigma_y \, \sigma_z)$ sec/m^3 ,

where

$\bar{u}$ = average wind speed (m/sec) ,

σ_y, σ_z = standard deviation of the plume distribution in the y and z directions (m).

F_d = depletion factor (due to ground deposition) for the radioactive cloud = Q'_x/Q'_o ,

where

Q'_x = effective depleted source term,
Q'_o = original source term.

The dilution and depletion factors, at selected downwind distances, for the three meteorological conditions of interest (see preceding section) are shown in Table C-II. The

dilution factors are from Hilsmeier and Gifford;[C8] the depletion factors are based on the work of Chamberlain.[C9]

Using K_x and F_d, the thyroid dose can be computed as follows.

$$D_T = (1/\pi \bar{u} \, \sigma_y \, \sigma_z) \, F_d \, R(\Sigma \, Q_n \, B_n) \text{ rads}$$

$$= K_x \, F_d \, R(\Sigma \, Q_n \, B_n) \text{ rads} ,$$

where

R = breathing rate = 3.47×10^{-4} m^3/sec ,

Q_n = curies of nth iodine nuclide released,

B_n = rads/curie of nth iodine nuclide inhaled.

In the equation above, $K_x \, Q_n$ is the concentration time integral for the nth iodine nuclide. Using this formula and

TABLE C-II

DILUTION FACTORS (K_x) VS DOWNWIND DISTANCES (X) FOR SELECTED STABILITY CATEGORIES
(Depletion factors F_d at a deposition velocity of 1 cm/sec, applicable to iodine isotopes, are given in parentheses.)

Downwind Distance (m)	Dilution Factor (Sec/m^3)		
	Type C, 5 m/Sec	Type E, 1 m/Sec	Type F, 1 m/Sec
100	8.0×10^{-4} (9.1×10^{-1})	2.1×10^{-2} (6.0×10^{-1})	5.0×10^{-2} (5.2×10^{-1})
200	2.0×10^{-4} (9.1×10^{-1})	5.3×10^{-3} (5.1×10^{-1})	1.2×10^{-2} (4.0×10^{-1})
400	6.0×10^{-5} (9.0×10^{-1})	1.4×10^{-3} (4.2×10^{-1})	3.3×10^{-3} (2.6×10^{-1})
800	1.5×10^{-5} (8.9×10^{-1})	4.5×10^{-4} (2.8×10^{-1})	9.3×10^{-4} (1.8×10^{-1})
1000	1.0×10^{-5} (8.8×10^{-1})	3.1×10^{-4} (2.7×10^{-1})	7.0×10^{-4} (1.5×10^{-1})
2000	2.8×10^{-6} (8.7×10^{-1})	1.0×10^{-4} (2.2×10^{-1})	2.2×10^{-4} (9.0×10^{-2})
3500	9.0×10^{-7} (8.6×10^{-1})	3.8×10^{-5} (1.7×10^{-1})	9.5×10^{-5} (5.5×10^{-2})
5000	5.2×10^{-7} (8.5×10^{-1})	2.5×10^{-5} (1.3×10^{-1})	6.0×10^{-5} (3.8×10^{-2})
10000	1.8×10^{-7} (8.2×10^{-1})	9.0×10^{-6} (7.4×10^{-2})	2.6×10^{-5} (1.4×10^{-2})

the data shown in Tables C-I and C-II, one can calculate the thyroid doses, shown in Table C-IV.

Because of the various possible iodine release fractions, the radioactive cloud doses were computed separately for the noble gases and for the iodines. The integrated dose due to the passage of a semi-infinite radioactive cloud[C9] is given by

$$D_\gamma = 0.25 \, (\rho_0/\rho) \, \overline{E}_\gamma \, \psi \text{ rads}$$

where

(ρ_0/ρ) = correction factor for air at other than standard conditions = 1.2 at 7000-ft altitude.

$\overline{E}_\gamma$ = average gamma energy (MeV) released per disintegration

ψ = concentration time integral (Ci-sec/m^3)

For the problem at hand, the contributions to the cloud dosage can be written as follows:

$$D_\gamma \text{ (Xe + Kr)} = 0.3 \, K_x \text{ (Ci-MeV/dis)}_{Xe+Kr} \text{ rads}$$

$$D_\gamma \text{ (iodines)} = 0.3 \, K_x \, F_d \text{ (Ci-MeV/dis)}_{iodines} \text{ rads}$$

Using the data given in Table C-II and the values of Ci-MeV/dis given in Table C-III, the cloud dosages were computed; the results for the Xe + Kr and iodine contributions are tabulated in Table C-IV.

It then remains to compute the gamma doses from the radioactive iodines deposited on the ground. For the assumed 0.01-m/sec deposition velocity, one can write

Deposition rate (Ci/m^2) =

(0.01 m/sec) x (ψ Ci – sec/m^3) ,

where ψ is the concentration time integral. Assuming infinite plane source geometry, the gamma dose rate contribution from the ith iodine nuclide ($D^i_{\gamma,t}$) was obtained for a detector point 1m above ground. The dose rate for infinite exposure, taking radioactive decay into account, can be shown to be ($D^i_{\gamma,t}/\lambda^i$), where λ^i is the appropriate disintegration constant. The total dose, obtained by summing the latter expression over the iodine nuclides, can also be corrected to account for the finite nature of the source; this was done, and the results are shown in Table C-IV.

5. Calculation of Individual Mortality Risks

The data in Table C-IV can now be used to obtain curves of individual mortality risk vs downwind distance (from the reactor) for each of three directions of interest, cross canyon, up canyon, and down canyon. Using the curve of atmospheric release vs accident probability per year (Fig. 2), we scaled the doses in Table C-IV (in a specified direction) appropriately to account for the release conditions associated with each postulated accident.

TABLE C-III

DATA USED IN DETERMINATION OF EFFECTIVE GAMMA-RAY SOURCE STRENGTH FOR WHOLE-BODY DOSE CALCULATIONS, BASED ON RELEASE FRACTION OF 1.0 FOR ALL NUCLIDES

Nuclide	Half-Life	Gamma MeV Per Dis	Curies Released/ Fuel Element	Ci-MeV/Dis
^{83m}Kr	1.9 H	0.041	1.14×10^3	4.67×10
^{85m}Kr	4.4 H	0.2	2.90×10^3	5.80×10^2
^{87}Kr	76. M	1.4	5.55×10^3	7.77×10^3
^{88}Kr	2.8 H	2.0	7.84×10^3	1.57×10^4
^{131}I	8.1 D	0.4	5.32×10^3	2.13×10^3
^{132}I	2.3 H	2.0	8.23×10^3	1.65×10^4
^{133}I	20.6 H	0.55	1.45×10^4	7.98×10^3
^{134}I	53. M	1.3	1.74×10^4	2.26×10^4
^{135}I	6.7 H	1.5	1.36×10^4	2.04×10^4
^{131m}Xe	12. D	0.163	4.26×10	6.94
^{133m}Xe	2.3 D	0.233	2.93×10^2	6.83×10
^{133}Xe	5.3 D	0.081	1.13×10^4	9.15×10^2
^{135m}Xe	16. M	0.52	4.10×10^3	2.13×10^3
^{135}Xe	9.1 H	0.25	1.41×10^4	3.53×10^3
^{138}Xe	17. M	1.0	1.23×10^4	1.23×10^4

TABLE C-IV

THYROID AND WHOLE-BODY GAMMA-RAY DOSES, IN RADS PER FUEL-ELEMENT
INVENTORY RELEASED, BASED ON RELEASE FRACTION OF 1.0 FOR ALL NUCLIDES
(GMA XE + KR) and (GMA IODINE) are doses from radioactive cloud.
GMA DEPOS) is dose from ground deposition of iodine.

Downwind Distance (meters)	Dose (Rads)/Fuel-Element Inventory Released		
	Type C, 5 M/Sec	Type E, 1 M/Sec	Type F, 1 M/Sec
100 (THYROID)	4.10E+03	7.10E+04	1.47E+05
(GMA XE+KR)	1.03E+01	2.71E+02	6.46E+02
(GMA IODINE)	1.52E+01	2.63E+02	5.43E+02
(GMA DEPOS)	1.18E+02	1.60E+03	2.70E+03
200 (THYROID)	1.03E+03	1.52E+04	2.70E+04
(GMA XE+KR)	2.58	6.84E+01	1.55E+02
(GMA IODINE)	3.80	5.64E+01	1.00E+02
(GMA DEPOS)	3.24E+01	4.38E+02	6.78E+02
400 (THYROID)	3.04E+02	3.32E+03	4.84E+03
(GMA XE+KR)	7.75E-01	1.81E+01	4.26E+01
(GMA IODINE)	1.13	1.23E+01	1.79E+01
(GMA DEPOS)	1.06E+01	1.05E+02	1.43E+02
800 (THYROID)	7.52E+01	7.10E+02	9.44E+02
(GMA XE+KR)	1.94E-01	5.81	1.20E+01
(GMA IODINE)	2.79E-01	2.63	3.50
(GMA DEPOS)	2.80	2.48E+01	3.16E+01
1000 (THYROID)	4.96E+01	4.72E+02	5.92E+02
(GMA XE+KR)	1.29E-01	4.00	9.04
(GMA IODINE)	1.84E-01	1.75	2.19
(GMA DEPOS)	1.87	1.70E+01	2.04E+01
2000 (THYROID)	1.37E+01	1.24E+02	1.12E+02
(GMA XE+KR)	3.62E-02	1.29	2.84
(GMA IODINE)	5.09E-02	4.59E-01	4.13E-01
(GMA DEPOS)	5.42E-01	4.68	4.12
3500 (THYROID)	4.36	3.64E+01	2.94E+01
(GMA XE+KR)	1.16E-02	4.91E-01	1.23
(GMA IODINE)	1.62E-02	1.35E-0'	1.09E-01
(GMA DEPOS)	1.75E-01	1.42	1.14
5000 (THYROID)	2.50	1.83E+01	1.29E+01
(GMA XE+KR)	6.71E-03	3.23E-01	7.75E-01
(GMA IODINE)	9.23E-03	5.79E-02	4.76E-02
(GMA DEPOS)	1.01E-01	7.22E-01	5.02E-01
10000 (THYROID)	8.32E-01	3.76	2.06
(GMA XE+KR)	2.32E-03	1.16E-01	3.36E-01
(GMA IODINE)	3.08E-03	1.39E-02	7.60E-03
(GMA DEPOS)	3.36E-02	1.51E-01	8.16E-02

The discussion in Sec. 2 above shows that, whereas the Xe-Kr dose contribution is directly proportional to the core fraction melted, the iodine contribution depends on which of three release modes was responsible for the release. Dose rates were converted to individual mortality risks as suggested by Otway.[C10] For radiation-induced thyroid carcinoma, we assumed a mortality risk of 1×10^{-6} per person per rad. For whole-body radiation, we assumed a risk estimate of 30×10^{-6} per person per rad up to 150 rad. Above 150 rad, the risk was based upon

the response to acute whole-body irradiation. Results of these calculations for the cross-canyon case at distances of 10^2, 10^3, and 10^4 m are shown in Figs. C-1 through C-3. Corresponding curves for the up- and down-canyon cases were also plotted. The individual mortality risk at a given distance was obtained by integrating the curve in question. Results of these integrations are shown in Figs. 3 through 5 in the body of the report. The method used to account for local meteorology and to infer lines of constant mortality risk (Fig. 6) is given in Appendix F.
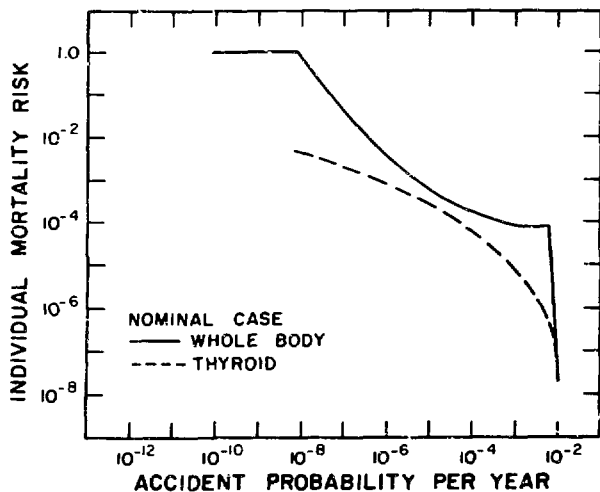

Fig. C-1.
Individual mortality risk vs accident probability at 10^2 meters. (Pasquill Condition Type C, 5 m/sec cross-canyon wind).
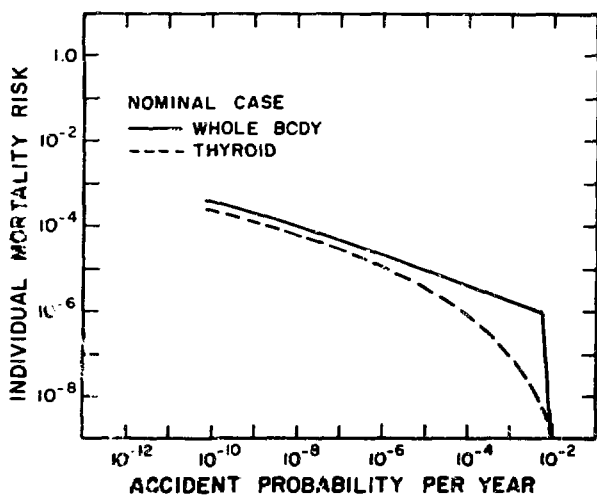

Fig. C-2.
Individual mortality risk vs accident probability at 10^3 meters. (Pasquill Condition Type C, 5 m/sec cross-canyon wind).
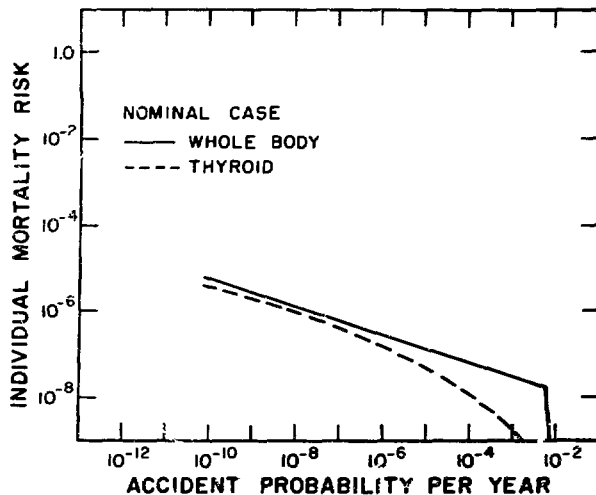

Fig. C-3.
Individual mortality risk vs accident probability at 10^4 meters. (Pasquill Condition Type C, 5 m/sec cross-canyon wind).

References

C 1. S. K. Penny, D. K. Trubey, and J. Gurney, "Bibliography, Subject Index, and Author Index of the Literature Examined by the Radiation Shielding Information Center," Oak Ridge National Laboratory report ORNL-RSIC-5 (Rev. 1) (1966), pp. 15-19.

C 2. J. F. Perkins and R. W. King, "Energy Release from the Decay of Fission Products," Nucl. Sci. Eng. 3, 726 (1958).

C 3. J. F. Perkins, "Decay of U-235 Fission Products," Redstone Arsenal report RR-TR-63-11 (1963).

C 4. K. O. Koebberling, W. E. Krull, and J. H. Wilson, "Lockheed Fission Product Inventory Code," Lockheed-Georgia Company Internal report ER-6906 (1964).

C 5. M. E. Battat, D. J. Dudziak, and H. R. Hicks, "Fission Product Release and Inventory from ^{239}Pu Fast Fission," Los Alamos Scientific Laboratory report LA 3954 (1968).

C 6. J. J. DiNunno, F. D. Anderson, R. E. Baker, and R. L. Waterfield, "Calculation of Distance Factors for Power and Test Reactor Sites," U. S. Atomic Energy Commission document TID-14844 (1962).

C 7. H. T. Williams, O. W. Stopinski, J. L. Yarnell, A. R. Lyle, C. L. Warner, and H. L. Maine, "1969 Status Report on the Omega West Reactor, with Revised Safety Analysis," Los Alamos Scientific Laboratory report LA-4192 (1969).

C 8. W. F. Hilsmeier and F. A. Gifford, Jr., "Graphs for Estimating Atmospheric Dispersion," Oak Ridge National Laboratory report ORO-545 (1962).

C 9. "Meteorology and Atomic Energy 1968," David H. Slade, Ed., U. S. Atomic Energy Commission/Division of Technical Information (1968), pp. 204-206.

C10. H. J. Otway, "The Application of Risk Allocation to Reactor Siting and Design," Los Alamos Scientific Laboratory report LA-4316 (1970).

APPENDIX D

SUMMARY OF RELIABILITY DATA

The failure rates for critical components and systems used in this analysis were derived from reliability measurements and estimates found in the literature and from statistical treatment of both OWR system test data and OWR (and other reactor) operating histories. References D1 through D4 were used as background for the following discussion of reliability estimates for important elements.

1. Main Coolant Line Failure

Measured failure-rate data for primary system piping are scarce, but there are many calculated and intuitive estimates in the literature. Values of 2×10^{-3} to 3×10^{-6}/yr have been reported[D5,D6] for large-scale rupture of primary coolant systems in various types of reactors. Otway,[D7] on the basis of a literature search, used 10^{-3}/yr as a pessimistic estimate for catastrophic failure of the primary coolant system of a pressurized water reactor (PWR). Green and Bourne[D5] estimated the reliability of hydraulic hoses and pressure vessels to be about a factor of ten higher for low-stress than for high-stress (pressure) applications. The OWR primary piping is schedule 10 (or greater) stainless steel which at $53°C$ maximum operating temperature would have an allowable working pressure (AWP) of about 350 psig. The AWP is based upon one-quarter of ultimate strength, so the pressure corresponding to ultimate strength would be about 1400 psig, whereas the maximum operating pressure in the OWR is 28 psig. Further, most of the OWR primary system is underground and not exposed to mechanical damage. Because of this and the very low operating pressure we have conservatively used 5×10^{-5}/yr as the probability of catastrophic rupture of the primary coolant system.

2. Instrument Port Failure

Although the five 4-in.-diam instrument ports that penetrate the reactor tank are considerably smaller than the main coolant line, their location below the reactor core warrants consideration of their possible role in loss-of-coolant accidents. Because of their close proximity to the core, these ports are exposed to high neutron and gamma fluxes; also, their location precludes inspection and testing once they are installed. For gas-cooled reactors, Cave and Holmes[D8] have proposed values for the probability of sudden and severe failure of steel pressure parts. Where there is no reinspection nor retesting, they give a failure probability of 10^{-4} in 30 yr of service for parts exposed to neutron irradiation; for unirradiated components, the figure is a factor of 10 smaller. Note that the instrument ports are exposed only to the static pressure from the water in the tank. For this study, we have used a failure rate of 5×10^{-4}/yr for the instrument ports, i.e., a factor of 10 higher than that assumed for the main coolant line.

3. Antisiphon System Failure

The main component of the antisiphon loop in the OWR is the "flapper" valve (see Appendix A). During normal cooling flow, this valve is closed; on loss of flow it falls open under its own weight. One method used to estimate the failure rate for this valve was based on OWR test data. The flapper valve in its present configuration has operated for approximately 13 yr without failure. During normal reactor operations the main coolant pump is turned off approximately once a week. If the flapper valve should fail to close on startup of the pump, the core coolant flow would be drastically reduced and the malfunction would be indicated by annunciator signals at the reactor console. Using a value of no failure in 500 observations, we estimate failure probabilities of 4.6×10^{-3}/demand (90% upper confidence limit) and 1.4×10^{-2}/demand (99.9% upper confidence limit).

Reliability may also be estimated by considering the valve as a component that is in continuous service and assigning it a failure rate. Failure rates quoted[D3] for various valve types (ball, butterfly, check, and control valves) range from 3 to 8 failures/10^6 h, or 0.03 to 0.07/yr. Because of the importance of this valve, we have used the conservative value of 7×10^{-2}/yr.

4. Emergency Core Spray System No. 1

This system uses city water from the fire water main. Decision to actuate this system is made by the operating crew and involves manipulation of two valves. The system is checked each week by an indirect functional test procedure. In assigning a failure probability, we used the following individual component probabilities.

Fire water main system	10^{-4}/demand
Valve failure rate	10^{-3}/demand
Operator error	10^{-3}/operation

Using the methods described in Appendix B, we computed the failure probability to be 2.1×10^{-3}/demand.

5. Emergency Core Spray System No. 2

T' 's system uses reactor-system water and employs an electrically driven pump to deliver cooling spray to the core. Therefore, the reliability depends only on the success or failure of the electric motor starter circuit. Probability of the electric motor's failing once started, was selected as 5×10^{-3}/yr,[D1, D3, D4] and the probability of startup failure was conservatively taken as 10 times the yearly failure rate, giving 5×10^{-2}/demand.

An alternate method was also used to estimate the spray system's reliability on the basis of OWR operating data. This system is routinely checked each week, and no failures have been observed in 130 checkouts. On the basis of Appendix B, the failure probabilities were computed as 1.8×10^{-2}/demand (90% upper confidence limit) and 5.2×10^{-2}/demand (99.9% upper confidence limit). The latter value, which compares with those in the literature, was used in the accident calculations.

6. Control Rods and Scram Systems

The control rods and reactor scram systems have not failed to respond to shutdown demand in the past 13 yr of OWR operation. An estimated 3200 scram demands have been initiated without failures. According to Appendix B, the failure probability is 7.2×10^{-4}/demand (90% upper confidence limit) and 2.2×10^{-3}/demand (99.9% upper confidence limit).

7. Cladding Defects in Fuel Elements

Harrison[D9] reports that in the first 11 yr of operation, the Materials Testing Reactor (MTR) successfully used over 2000 MTR-type fuel-element assemblies. However, on three separate occasions, mechanical deficiencies in the assemblies were responsible for 164 to 184 "failures." On only one of these occasions, when 142 failures were caused by a seemingly minor change in assembly design, did the cladding rupture or any fissile material or fission products escape from the fuel plates. The other failures were caused by undetected errors during assembly fabrication. Eagan[D10] has reported multiple failures of cladding on MTR-type fuel elements over a 2-yr period.

During this period, three different companies manufactured the reactor fuel, but only that from one manufacturer failed. Before this 2-yr period, the reactor had operated for 9 yr without any cladding failure. In light of these experiences, it seemed reasonable to assign a cladding failure probability based on the OWR experience of no cladding failures during 13 yr of operation. Using these data, one arrives at 0.2 to 0.5/yr for the 90% and 99.9% upper confidence limits, respectively. A value of 0.5/yr was chosen for this study.

References

D 1. "Failure Data Handbook for Nuclear Power Facilities," Liquid Metals Engineering Center report LMEC-MEMO-69-7 (1969).

D 2. "Failure Rate Data Book," Vols. 1-3, U. S. Naval Fleet Missile Systems and Evaluation Group, Corona, California, 1966-1960.

D 3. "Reliability Analysis of Nuclear Power Plant Protective Systems," Holmes and Narver report HN-190 (1967).

D 4. Earles, "Reliability Application and Analysis Guide," MI-60-54 (Rev. 1), The Martin Company (July 1961).

D 5. A. E. Green and A. J. Bourne, "Safety Assessment with Reference to Automatic Protective Systems for Nuclear Reactors," AHSB-(S)-117 (1966).

D 6. L. Cave and J. R. Crickmer, "Safety Assessment of Fast Reactors by Probability Methods," Proc. Intern. Conf. Safety of Fast Reactors, Aix-en-Provence, France, September 1967.

D 7. H. J. Otway, "The Application of Risk Allocation to Reactor Siting and Design," Los Alamos Scientific Laboratory report LA-4316 (1970).

D 8. L. Cave and R. E. Holmes, "Suitability of the Advanced Gas-Cooled Reactor for Urban Siting," Proc. Symp. Containment and Siting of Nuclear Power Plants, Vienna, April 1967.

D 9. L. J. Harrison, "Mechanical Failures of MTR Fuel Assemblies," Nucleonics 21, No. 10, 78 (1963).

D10. J. L. Eagan, "Multiple Failures of MTR-Type Fuel Elements at the LPTR," University of California Research Laboratory report UCRL-71736 (1969).

APPENDIX E

SUMMARY OF ACCIDENTS CONSIDERED

1. Introduction

Estimation of numerical reliability values for reactor systems and components is important in probabilistic reactor risk analysis. The reliability data are used to obtain overall probabilities for postulated accidents. The accident probabilities, together with their associated consequences, are the input to the risk calculation. Here, we will examine several accidents, compute their probabilities, and give release estimates. For those accidents which do result in a fission-product release, the computed probabilities and release figures provide the input data for the dispersion and dose calculations discussed in Appendix C.

Accidents which could result in fission-product release to the atmosphere may be categorized as reactivity accidents, loss of coolant, loss of cooling flow, and fuel element cladding failures. In the analysis of these accidents, the engineered safeguards and safety systems incorporated in the Omega West Reactor (OWR) design are important considerations. These safety features include an antisiphon loop, a free convection loop, two emergency core spray systems, control-rod design compatible with both safety and operational requirements, and safety system instrumentation (see Appendix A). The fission-product releases quoted in this appendix are in terms of curies of ^{131}I released. However, in performing the dispersion and dose calculations, due account is taken of the other iodine isotopes and the Xe-Kr fission products.

2. Reactivity Accidents

The reactivity accidents chosen for this study have been discussed by Williams et al. in the 1969 status report on the OWR,[E1] so only brief descriptions of selected accidents are given here. These include control-rod breakage, startup accidents, accidents at power, and core loading accidents. Williams and co-workers also considered accidental reactivity additions due to manual withdrawal of the control rods and replacement of air with water (or graphite) in the experimental ports, but concluded that these did not pose any safety problems. In fact, from results of SPERT experiments for OWR-like cores, Williams and co-workers concluded that only a core loading accident could result in fission-product release. For the OWR, the SPERT results indicated that periods shorter than 4 to 5 msec would be required to produce fuel melting.

(a) Control Rod Breakage. A reactivity excursion could result if one of the control rods broke accidentally

and the absorber section moved from a region of higher to a region of lower worth. The maximum step increase in reactivity due to a rod break, from a 10-kW initial power level, is estimated as 1% in $\Delta k/k$, corresponding to a 22-msec period. Considering SPERT data, the excursion would be self-limiting with maximum fuel temperatures of 150°C, and no fission products would be released.

(b) Startup Accidents. A possible consequence of an operator error, or control-rod drive failure, or both is the sequential or simultaneous withdrawal of the control rods. During startup, and for an initial power level of 0.8 W (apparent source level), the following values were calculated. For sequential withdrawal at maximum speed, the ramp rate is 0.16 $/sec and the minimum period is 63 msec. In case of simultaneous withdrawal of all eight control rods, the maximum reactivity insertion rate would be 0.8 $/sec with a minimum period of 21 msec. These minimum values are larger than the 4- to 5-msec periods required for fuel melting. The probability of a reactivity fault at startup, due to either equipment failure or operator error, is of the order of 10^{-4} per year.[E2]

(c) Accidents During Power Operation. In the OWR, an automatic control system is used to hold the reactor power constant at any preset level from 10 kW to design power. This is accomplished by a servo system that drives the four central control rods and is so designed that the maximum reactivity rate for the four rods moving together is about 0.004 $/sec. Results of tests that simulated the reactor response to a continuous rod withdrawal by the servo system showed a two-decade increase in power level over 130 sec, with a final reactor period longer than 10 sec. Because of the slow response, sufficient time is available for operator action or for one of the scram channels to terminate the power rise before reactor damage can occur. Reactor faulting at power has been estimated as 10^{-2} per year.[E2]

(d) Core Loading Accident. The core loading accident discussed by Williams et al.[E1] was the dropping of a fuel element in a just-critical core. They estimated that this would result in (1) a ramp reactivity-insertion rate of 10 $/sec, (2) a minimum period of 4.7 msec, (3) melting of about 2% of the total fuel plate area, and (4) escape to the atmosphere of less than 0.01% of the iodines. They also stated that such an accident could only result from multiple mistakes and accidental deviations from carefully controlled procedures.

For a core loading accident to occur, a fuel loading operation must have preceded the reactor startup; denote

this probability by P_L. If the reactor is in operation for 6240 h/yr (120 h/wk) and we assume that the refueling operations require a total of 100 h/yr, P_L is (100/6240) or 1.6×10^{-2}/yr. We will also conservatively assume that only two procedural errors are required to initiate such an accident. The probability of any given instruction's being executed improperly, or being omitted, is given by Otway[E2] as 10^{-3} to 10^{-4} per instruction. Using 10^{-3}, the overall accident probability is 1.6×10^{-8}/yr; the release (0.01% of the iodines) is 16.5 Ci of ^{131}I and accompanying fission products. Note that the OWR has a fuel element hold-down grid to prevent inadvertent lifting of any fuel element from the matrix. This grid is unlocked and lifted aside during core loading.

3. Loss-of-Coolant Accidents

The severity of a loss-of-coolant accident is primarily a function of the time (after shutdown) required for the coolant level to drop below the core. The time to drain the tank depends, in turn, on whether the reactor tank lid is open or closed. During normal operation, it is closed, but loss of integrity of any one of its various penetrations (including two access hatches) would amount to its being open. Williams et al.[E1] present data which show that fuel melting will occur only if the tank is drained below the level of the core less than 30 min after shutdown without corrective measures being taken. Loss-of-coolant accidents considered here are a main coolant line rupture and an instrument port rupture (see Appendix A). Appendix D contains a discussion of the reliability data used in the following analysis.

(a) **Main Coolant Line Rupture.** The most severe loss-of-coolant accident is postulated to be a guillotine break of the main coolant line, with the reactor top open and all the engineered safeguard systems failed. The systems of interest for this accident chain are the antisiphon loop (flapper valve) and emergency core-spray system No. 1. In case of a main line break, emergency core-spray system No. 2 is not taken as a sequence in the accident chain because its source of water is the delay line which is part of the primary loop. Failure rates used in arriving at the overall accident probability are shown in Table E-1. Also shown are the corresponding figures for the case with the tank top closed and the 90% upper confidence limits.

The consequences of these accidents, in terms of fission-product release, are difficult to assess. With the tank top open, the extent of fuel melting is an extremely sensitive function of the time required to drain the tank. The fraction (approximately 2/3) of the core assumed to have melted is extremely pessimistic, but it seemed that that fraction would comfortably accommodate any possible mechanism that would drain the tank in a very few minutes. The figure of five fuel assemblies melted with the tank top closed reflects the longer time needed to drain the tank. The ^{131}I release to the atmosphere was based on the inventory calculations in Appendix C; a 50% iodine release from the melt and a 50% plate-out are included in the figures shown in Table E-1.

(b) **Instrument Port Rupture.** The OWR tank contains a number of penetrations that could either fail or rupture during an accident. In contrast to the rupture of a large-diameter (10 or 12 in.) main coolant line, a break in one of these penetrations would probably create an effective drainage aperture about 4 in. in diameter.[E1] Taking an instrument port break as a typical example, the time to drain the tank below core level is estimated as 6 min if the reactor tank top is open. With the top closed, the drainage time would be considerably longer.[E1]

Given an instrument port rupture, the engineered safeguards to be considered are the two emergency core-spray systems. Assuming the reactor tank top to be open, the sequences in the accident chain are as follows:

(1) Probability of an instrument port rupture, 5×10^{-4}/yr.

(2) Reactor tank top open, 10^{-2}/yr.

(3) Core-spray system No. 1 failure, 2.1×10^{-3}/demand.

(4) Core-spray system No. 2 failure, 5.2×10^{-2}/demand.

Thus, the accident probability for an instrument port rupture (tank top open) is 5.5×10^{-10}/yr. The consequence of such an accident is estimated to be a melting of 10% (three fuel assemblies) of the core. Using a 50% iodine release from the melt and 50% plate-out, this corresponds to an ^{131}I release of 4×10^3 Ci. The value used by Williams et al.[E1] for a similar case was 2.7×10^3 Ci of ^{131}I released. With the reactor tank top closed, the accident probability is 5.5×10^{-8}/yr and the assumed ^{131}I release is 6.7×10^2 Ci, corresponding to meltdown of half a fuel assembly.

4. Loss of Cooling Flow

This group of accidents includes those that do not involve rupture of the coolant piping. Failure of the primary coolant pump and loss of flow through the individual fuel elements have been analyzed as the most probable accidents in this category.

(a) **Loss of Main Coolant Pump.** The power level at which the OWR operates and the automatic convective loop incorporated in its design protect the core in case of main coolant pump failure. Even without the automatic convective loop, the flow passages between the upper tank and the plenum below the core aid in setting up a natural convective path. The efficacy of the automatic convective loop has been demonstrated by experimental

ACCIDENT PROBABILITIES AND ^{131}I RELEASES FOR LOSS-OF-COOLANT ACCIDENTS
(Figures in parentheses are 90% upper confidence limits.)

	Tank Top Open	Tank Top Closed	Units
Failure Rates			
Main-Line Rupture	5×10^{-5} (1.9×10^{-4})	5×10^{-5} (1.9×10^{-4})	Per year
Flapper Valve	7×10^{-2} (2.5×10^{-1})	7×10^{-2} (2.5×10^{-1})	Per year
Vessel Top	1×10^{-2} (3.9×10^{-2})	9.9×10^{-1} ($9. \times 10^{-1}$)	Per year
Core-spray No. 1	2.1×10^{-3} (8.2×10^{-3})	2.1×10^{-3} (8.2×10^{-3})	Per demand
Overall Accident Probability	7.3×10^{-11} (1.5×10^{-8})	7.3×10^{-9}	Per year
Fission-Product Release			
Fuel Assemblies Melted	20	5	Per accident
[131]I Release	2.7×10^{4}	6.7×10^{3}	Curies

tests which showed that the maximum fuel surface temperature attained under this circumstance was about 100°C.

(b) **Fuel-Element Flow Blockage.** Experience with reactors employing Materials Testing Reactor (MTR) fuel assemblies has shown that flow blockage from foreign material entrained in the coolant is a possibility. In fact, it has been estimated that about 80% of all reactors have had foreign objects in their coolant systems at one time or another.[E3] In 500 reactor-years of operating history, flow blockage accidents (with some fission-product release) have occurred in at least three reactors of the same general type as the OWR.[E1]

The above information implies that the probability of a blockage is (3/500) or 0.006/yr. Assuming that the number of fuel assemblies blocked is represented by a binomial distribution, the probability of X fuel assemblies being blocked is

$$P(X) = \frac{N!}{X!(N-X)!} p^X (1-p)^{N-X} \quad ,$$

where
N = total number (31) of fuel assemblies,

P = probability that a fuel assembly is blocked,
X = the number of fuel assemblies blocked.

Thus

$$P(0) = 1.0 - 0.006 = (1-p)^{31} \quad ,$$

from which $p = 1.94 \times 10^{-4}$. With this information, one can solve for P(X) as follows.

$$P(1) = 5.98 \times 10^{-3} \text{ blockage/yr},$$

$$P(2) = 1.74 \times 10^{-5},$$

$$P(3) = 3.26 \times 10^{-8},$$

$$P(4) = 4.43 \times 10^{-11}.$$

Blockage involving more than three fuel elements was not considered for this analysis.

If fuel melting occurs because of flow blockage, the magnitude of the iodine release depends on whether the discharge is directly to the atmosphere or through the stack filters. Venting through the filters requires that the reactor operator switch a vent valve. Either operator error or valve failure causes the sequence to fail. Assuming

10^{-3}/demand operator error and 2.5×10^{-2}/demand valve failure (estimated from OWR test experience), the combined failure rate is 2.6×10^{-2}/demand. Hence, the probability of direct release to the atmosphere is 0.026 P(X)/yr. Conversely, the probability of venting through the stack filters is $(1 - 0.026)$ P(X)/yr.

For the fuel blockage accidents we assume, first, blockage of 1, 2, or 3 fuel assemblies resulting in melting of 1/4, 1, or 3 fuel assemblies, and, second, a 50% iodine release from the melt to the water and a 10% iodine release from the water to the atmosphere. For venting through the stack filters, we applied a reduction factor of 10^2 to the iodine release, based on a 99% filter efficiency. It is also convenient to define

AP(X) = accident probability associated with blockage of X fuel assemblies,

AR(X) = ^{131}I release corresponding to AP(X).

With the above assumptions and definitions, the values of AP(X) and AR(X) for direct release to the atmosphere are

AP(1) = 1.6×10^{-4}/yr   AR(1) = 6.7×10 Ci ^{131}I
AP(2) = 4.5×10^{-7}/yr   AR(2) = 2.7×10^2 Ci ^{131}I
AP(3) = 8.4×10^{-10}/yr   AR(3) = 8.0×10^2 Ci ^{131}I.

For venting through the stack filters, the corresponding figures are

AP(1) = 5.8×10^{-3}/yr   AR(1) = 6.7×10^{-1} Ci ^{131}I
AP(2) = 1.7×10^{-5}/yr   AR(2) = 2.7×10^{-1} Ci ^{131}I
AP(3) = 3.1×10^{-8}/yr   AR(3) = 8.0×10^{-1} Ci ^{131}I

5. Defective Fuel Element Cladding

For this accident, the cladding failure rate was taken as 0.5/yr. As in Sec. 4(b) above, a value of 0.026/demand was assumed for the operator error plus valve failure sequence, and direct release to the atmosphere was assumed. The accident probability is thus 1.3×10^{-2}/yr. The release mechanism postulated for this accident was a cladding failure due to faulty fabrication or corrosion. Fission products considered were Xe, Kr, and, because of their high volatility, the iodine isotopes. If we assume that a cladding failure will expose 0.01% of the surface area of a fuel assembly (equivalent to the area of a 1/2-in.-radius circle) and that 0.01% of the iodine inventory per fuel assembly is released, the ^{131}I release is 2.7×10^{-2} Ci. This figure is based on a 50% release from the melt to the water and a 10% release from the water to the atmosphere.

References

E1. H. T. Williams, O. W. Stopinski, J. L. Yarnell, A. R. Lyle, C. L. Warner, and H. L. Maine, "1969 Status Report on the Omega West Reactor, with Revised Safety Analysis," Los Alamos Scientific Laboratory report LA-4192 (1969).

E2. H. J. Otway, "The Application of Risk Allocation to Reactor Siting and Design," Los Alamos Scientific Laboratory report LA-4316 (1970).

E3. R. E. Meuller, "Objects Found in Power Reactor Systems," American Nuclear Society Transactions, Supplement to Vol. 12 (October 1, 1969).

APPENDIX F

LOCAL METEOROLOGY

The location of the Omega West Reactor at the bottom of a long, deep canyon presents some unique problems in evaluating the risk to the surrounding population in case of fission-product release. For example, if inversion conditions exist in the canyon, the resulting suppression of vertical air movement will inhibit escape of effluent to the adjacent mesa tops. Thus, the canyon meteorology will determine the dispersion of an effluent cloud. On the other hand, if effluent is transported to the mesa top, the conditions at that level will govern its dispersion. Given a noninversion condition in the canyon, Stopinski[F1] has suggested that effluent transport to the

mesa top would require a northerly or southerly wind on the mesa and a wind of $180 \pm 60°$ (or $0 \pm 60°$) at the reactor site. Note that the canyon runs east-west and that most of the residential areas are north and west of the reactor site. To provide data for the OWR safety analysis, Stopinski[F1] studied the meteorology in the vicinity of the OWR. Data taken from March 15 to July 31, 1968, were tabulated, and those observations were selected which showed (1) a southerly wind component on the mesa, (2) winds of $180 \pm 60°$ at the reactor site, and (3) an isothermal or positive lapse rate from the floor of the canyon to its rim. Of a total of 2710 data points, 100, or 3.7%, met these criteria.

We used Stopinski's data to infer the probability of a noninversion condition in the canyon, where

P[Dose North] =

$$\frac{P[Noninversion]\quad P[Wind\ to\ North]}{P[Wind\ to\ North]\ +\ P[Wind\ to\ South]}$$

From the wind-rose data given in Table IX of the OWR status report,[F2] we infer that the probabilities of mesa winds in the $180 \pm 60°$ and $0 \pm 60°$ directions are 0.395 and 0.180, respectively. Using these figures, we obtain

P[Noninversion] = (0.037/0.395)(0.395 + 0.180) = 0.054.

Taking the reactor location as a reference point, and again using the wind-rose data, one can compute the probability (P_s) of the mesa winds blowing into a given sector. These computations indicate that P_s for the cross-canyon sectors

$(0 \pm 75°, 120 \pm 75°)$ is 0.688 and P_s for the up- and down-canyon directions $(90 \pm 15°, 180 \pm 15°)$ is 0.121. The probability of a calm period is 0.191. Defining P[sector] as the probability of fission-product transport to a given sector on the mesa, it follows that

$$P[sector] = (P_s/0.688)\ (0.054).$$

The values computed for P[sector] can be applied, as scale factors, to the appropriate individual mortality risk vs downwind distance curve (Fig. 3 in text) to obtain the distances corresponding to specified risk numbers. Results of this procedure are shown in Table F-I.

These data, together with results of similar calculations for the up- and down-canyon cases, can be graphically displayed by constructing lines of constant mortality risk on a schematic plan of the surrounding area (see Fig. 6 in the body of this report).

References

F1. O. W. Stopinski, "Interim Report on Winds in Los Alamos Canyon," LASL internal memorandum (September 25, 1968).

F2. H. T. Williams, O. W. Stopinski, J. L. Yarnell, A. R. Lyle, C. L. Warner, and H. L. Maine, "1969 Status Report on the Omega West Reactor, with Revised Safety Analysis," Los Alamos Scientific Laboratory report LA-4192 (1969).

TABLE F-I

CROSS-CANYON RISK PER SECTOR

Sector Angle (0° = N)	P[sector]	Mortality Risk vs Distance (m)			
		10^9/yr	10^{-10}/yr	10^{-11}/yr	10^{-12}/yr
105 to 150°	0.0057	210	690	2300	9000
150 to 195°	0.0057	210	690	2300	9000
195 to 255°	0.0068	230	750	2600	10000
285 to 330°	0.0052	200	650	2200	8500
330 to 015°	0.0163	350	1180	4200	18500
015 to 075°	0.0144	345	1150	4150	18400